

https://dspace.org/

The effect of a floating conductor on the breakdown performance of a non-uniform air gap under HVDC stress at both polarities

Hart, Craig L

2013-07-19
http://hdl.handle.net/10539/12850

Downloaded from a DSpace repository. https://dspace.org/

THE EFFECT OF A FLOATING CONDUCTOR ON THE BREAKDOWN PERFORMANCE OF A NON-UNIFORM AIR GAP UNDER HVDC STRESS AT BOTH POLARITIES

Craig L. Hart

A dissertation submitted to the Faculty of Engineering and the Built Environment, University of the Witwatersrand, Johannesburg, in fulfilment of the requirements for the degree of Master of Science in Engineering.

Johannesburg, 2013

Declaration

I declare that this dissertation is my own, unaided work, other than where specifically acknowledged. It is being submitted for the degree of Master of Science in Engineering in the University of the Witwatersrand, Johannesburg. It has not been submitted before for any degree or examination in any other university.

Signed this _____ day of _____ 2013

_____

Craig L. Hart

Abstract

A model for predicting the effect of a Floating Conductor (FC) on the breakdown voltage is presented and critically analysed in conjunction with results from laboratory work. Firstly, the scenario of live-line maintenance on HVDC lines is modelled by a FC within a rod-plane gap. The use of a rod-plane gap is to produce a non-uniform field distribution, representing the non-uniform field that would surround the conductor of a transmission line. This test object is then further simplified into simple gap geometries such that the breakdown voltage of the two gaps separated by the FC can be numerically calculated and the breakdown voltage of the entire test object predicted. The DC breakdown voltage of the rod-plane gap is then presented as a function of the position of the FC in the gap. The simulations are performed for both positive and negative DC voltages. The laboratory work uses a similar test object, with the U_{50} breakdown voltage recorded as a function of the position of the FC within the rod-plane gap. The simulation model is then critically analysed by comparing the laboratory and simulation results. It is concluded that although the model predicts the change in the breakdown strength from the starting to the ending points, the developed model has omitted detail that leads to discrepancies in the predicted results when compared to the laboratory results. This omitted detail includes the effect of corona discharge from the FC, additional parameters affecting the potential of the FC, the oversimplification of the gap geometry for numerical calculation, and the lack of a dynamic model for the changing electrostatic scenario as an applied voltage increases towards the breakdown voltage. The results also show that the position of a FC affects the breakdown strength of a non-uniform gap. This effect is due to the polarity dependent nature of breakdown in a non-uniform gap and in particular, the difference in the breakdown strength of a quasi-symmetrical (rod-rod) and asymmetrical (rod-plane) non-uniform gap. The effects of charged particles and their interaction with the floating conductor in the gap is also deemed to have a significant effect on the breakdown strength, with their behaviour also influenced by the sustained electric field that is a result of HVDC stress.

Acknowledgements

I would like to acknowledge all those within the School of Electrical & Information Engineering who have always offered assistance when it was needed. As a special mention, I would like to thank Mr Mark Goosens and Mr Harry Fellows for their assistance in putting together my laboratory set-up and support in the HV Lab.

I then would like to acknowledge the academic staff, who gave me my foundations during my undergraduate degree and then allowed me to build on it as a postgraduate. I would like to thank Prof. Ken Nixon for his guidance and support as my mentor, allowing me to challenge myself throughout my research. I would also like to thank Prof. Ian Jandrell for his support at the helm of the High Voltage research programme.

Then, I would like to acknowledge and thank my parents as they gave me the opportunity to study and then the freedom to continue.

I would gratefully like to acknowledge the following organisations for their funding and support:

- Eskom through the Tertiary Education Support Programme
- The National Research Foundation (NRF) for supporting the High Voltage research programme at Wits
- The Department of Trade and Industry (DTI) for Technology and Human Resources for Industry Programme (THRIP) funding.

The financial assistance of the National Research Foundation (NRF) towards this research is hereby acknowledged. Opinions expressed and conclusions arrived at, are those of the author and are not necessarily to be attributed to the NRF.

Contents

Declaration ii

Abstract iii

Acknowledgements iv

Contents v

List of Figures viii

List of Tables x

1 Introduction 1

2 Background 4

2.1 DC field conditions 4

2.2 DC breakdown: streamer and leader mechanisms 5

2.3 Previous research 6

2.3.1 Live-line maintenance 6

2.3.2 The breakdown performance of DC gaps 8

2.3.3 The effect of floating conductors in a DC field 9

2.4 Scope of the dissertation 9

3 Adopted approach 11

3.1 Problem statement 11

3.2 Overall approach taken 12

3.3 Modelling and simulations 12

3.4 Laboratory work 13

4 Modelling and simulations 14

4.1 Model of the live-line maintenance scenerio 14

4.2 Simplified gap geometry model 15
4.2.1 Positive polarity and non-inverted FC 16
4.2.2 Negative polarity and inverted FC 16
4.3 Capacitive modelling of the floating potential 17
4.4 Estimation of breakdown 20
4.4.1 Assumptions and limitations of the model and simulations . . 22
4.5 Simulation results 24

5 Laboratory work 27
5.1 Testing facility 27
5.2 Laboratory set-up 28
5.2.1 Generator 28
5.2.2 Rod-plane test gap 29
5.2.3 Floating conductor 30
5.3 Methodology 31
5.4 Laboratory results 32

6 Analysis and discussion 35
6.1 Overview of the laboratory results 35
6.1.1 Positive polarity 36
6.1.2 Negative polarity 37
6.2 Overview of simulation results and the model 39
6.3 Shortcomings of the model 41
6.3.1 Additional parameters affecting the floating potential 42
6.3.2 Geometry simplification 42
6.3.3 Absent effect of corona and pre-breakdown discharges 44
6.3.4 The lack of dynamic electrostatic scenario 45

7 Conclusions and recommendations 46
7.1 Recommendations 46
7.2 Conclusion 47

References 49

Bibliography 52

A Complete set of results from laboratory work 55

B Simulation script **60**

C Conference submission to ISH 2011 **69**

D Conference submission to PowerAfrica 2012 **75**

E Conference submission to GD 2012 **81**

List of Figures

2.1 High-speed photography of the DC breakdown of a rod-plane gap with a (a) 350 mm gap under positive DC stress and (b) 250 mm gap under negative DC stress 7

4.1 Diagram of the test object used to model the live-line working scenario for (a) Positive polarity and (b) Negative polarity 15

4.2 The simulation model of the test object for tests with a non-inverted floating conductor 16

4.3 The simulation model of the test object for tests with an inverted floating conductor 17

4.4 The test object in terms of capacitive relationships 18

4.5 The algorithm used for prediction of the breakdown voltage of the rod-plane gap with a floating conductor 23

4.6 Predicted breakdown strength of a positive DC gap with floating conductor as a function of the position of the floating conductor . . 26

4.7 Predicted breakdown strength of a negative DC gap with floating conductor as a function of the position of the floating conductor . . 26

5.1 Photograph of the test set-up used during laboratory work in the HV Lab at the the University of the Witwatersrand 28

5.2 Still from a video of flashover over the circuit of the DC generator in the HV Lab at the University of the Witwatersrand 29

5.3 Diagram of the test set-up used for laboratory work with (a) Positive polarity and (b) Negative polarity 30

5.4 The laboratory procedure during the laboratory work 31

5.5 U_{50} breakdown voltage (corrected for standard environmental conditions) of a positive DC rod-plane gap with a floating conductor with (a) $d_1 + d_2 = 80$ cm and (b) $d_1 + d_2 = 50$ cm 33

5.6 U_{50} breakdown voltage (corrected for standard environmental conditions) of a negative DC rod-plane gap with an inverted floating conductor with (a) $d_1 + d_2 = 25$ cm and (b) $d_1 + d_2 = 17.5$ cm . 34

6.1 Overview of the positive polarity results for both test gap sizes . . . 37
6.2 Overview of the negative polarity results for both test gap sizes . . . 38
6.3 Predicted and observed breakdown strength of a positive DC gap with a floating conductor as a function of the position of the floating conductor 40
6.4 Predicted and observed breakdown strength of a negative DC gap with a floating conductor as a function of the position of the floating conductor 41

List of Tables

4.1 Position nomenclature for the positive polarity test set-up 25
4.2 Position nomenclature for the negative polarity test set-up 25
6.1 The maximum change in the breakdown strength of the DC test gaps with the introduction of a floating conductor 36
6.2 Number of breakdowns at each level for the case of two distinct U_{50} levels in three negative polarity tests 39
6.3 Approximate decline of the breakdown strength of a positive DC rod-plane gap (100 mm) as a function of rod diameter and the field efficiency factor [1] 43
A.1 Results, environmental conditions and calculated correction factor for laboratory work with a positive DC voltage and a 500 mm air gap . 55
A.2 Results, environmental conditions and calculated correction factor for laboratory work with a negative DC voltage and a 175 mm air gap . 56
A.3 Results, environmental conditions and calculated correction factor for laboratory work with a negative DC voltage and a 175 mm air gap . 57
A.4 Results, environmental conditions and calculated correction factor for laboratory work with a negative DC voltage and a 175 mm air gap . 58

Chapter 1

Introduction

Worldwide, many power utilities perform live-line maintenance on their power transmission and distribution networks in order to minimise downtime and maximise power throughput on the network. Although individual power utilities set the guidelines for the practice of live-line maintenance on their networks, there are general guidelines that have been developed by working groups such as a those in CIGRE that discuss the technical requirements of its performance [2]. The Insitute of Electrical and Electronic Engineers (IEEE) also have a document pertaining to the performance of live-line maintenance [3]. The shortcoming of these documents is that to date, they have not specifically considered the implementation of live-line working on DC lines.

The nature of power transmission is now shifting from traditional AC networks toward the additional use of High Voltage Direct Current (HVDC) transmission networks. The number of proposed HVDC projects worldwide, as well as in Africa, is due to it being economical for power transmission over long distances when compared to High Voltage Alternating Current (HVAC) power distribution [4]. Renewable energy projects, such as hydroelectric plants, wind farms and solar plants are being proposed and constructed in specific locations due to prevailing conditions, and this results in vast distances between the generation and load. As an example, the distance to import power to South Africa from the Inga hydroelectric project would require close to 4000 km of transmission line, which is only realistically feasible by use of HVDC transmission lines [4].

Existing HVDC infrastructure can be found worldwide, and in South Africa there is the Cahora Bassa line which runs 1400 km from the Cahora Bassa dam in Mozambique to the Apollo converter station in Johannesburg and is responsible for

importing 1800 MW of hydroelectric power into South Africa (SA) [5]. Additionally in Southern Africa, there is the Caprivi Link in Namibia, which imports 350 MW of power from Zambia [6]. In addition to these two active HVDC lines in Southern Africa, there are also currently eight proposed HVDC transmission lines in Eskom's latest Transmission Development Plan (TDP) for 2012-2021. There are also five HVDC line projects that are currently deferred but still planned, including an 800 kV line from Lephale in Limpopo to Durban [7].

The benefits of HVDC transmission should now be combined with the advantages which live-line maintenance brings to the field of power transmission. Nonetheless, as with any aspect of high voltage engineering, safety is paramount and so such a scheme can only be attempted with a greater understanding of the physical nature of HVDC live-line maintenance.

As a fundamental approach to achieve such an understanding, this dissertation presents an investigation into the effect of a Floating Conductor (FC) on the breakdown strength of a non-uniform air gap under HVDC stress. The use of a FC in a non-uniform air gap models several scenarios of live-line working during which a metallic object is introduced between the live-line and a earthed structure, such as a tower. The investigation includes the development of a numerical-based model and simulations, confirmation of this model through laboratory work and an analysis of the fundamental physics relating to the breakdown of air insulation.

The structure of the dissertation is as follows:

Chapter 2: The field conditions surrounding a HVDC line are discussed, before an analysis of the DC breakdown mechanisms of air. Previous research that can relate to the topic of HVDC live-line maintenance is then presented before the scope of the dissertation is defined.

Chapter 3: The problem that is addressed in the dissertation is presented with the adopted approach to the research. A brief overview of this approach and its components (experimental and simulation work) is then given.

Chapter 4: The simulation component of the research is discussed in detail. The model used for simulations is introduced and discussed. The electrostatic analysis of the model is then presented, with the method for calculation of the floating potential of the floating conductor as well as the estimation of breakdown. Lastly, the results of the simulations are presented.

Chapter 5: The laboratory component of the research is discussed in detail. This includes an overview of the testing facility used, the experimental set-up in the laboratory and the general methodology. Lastly, the results of the laboratory work are presented.

Chapter 6: The results from both components of the research are analysed. This includes an in-depth analysis of the laboratory results in isolation of the simulation results, before an overview of the simulation results. The two sets of results are then compared and analysed, with the validity of the developed model discussed.

Chapter 7: Recommendations for future work towards the presented research are given. The conclusions drawn from the presented research are summarised.

Appendix A: A complete set of the results obtained during experimental work is presented, along with the environmental conditions that each test was conducted in.

Appendix B: The implementation of the simulation work within MATLAB and femm 4.2 is presented. This acts as a supplement for **Chapter 4**.

Appendix C: A paper by the author that contributes towards **Chapter 2** is included. This paper was presented at the 17^{th} International Symposium on High Voltage Engineering (ISH) in 2011 and can also be found in the conference proceedings.

Appendix D: A paper by the author that is based on the presented work is included. This paper was presented at IEE PES Power Africa 2012.

Appendix E: A paper by the author that is based on the presented work is included. This paper was presented at 19^{th} International Conference on Gas Discharges and Their Applications in 2012 and can also be found in the conference proceedings.

In the following chapter, the field conditions surrounding an HVDC line and the mechanisms of DC breakdown are outlined. Previous research into relative topics for the scope of this dissertation is then discussed.

Chapter 2

Background

Background on the field conditions surrounding HVDC lines and the mechanisms of DC breakdown are given. Previous research that relates to the topic of HVDC live-line maintenance is discussed. The previous research that was considered relevant includes work relating to live-line maintenance on HVAC lines, the breakdown performance of air gaps stressed by DC voltages, and research that looked at the effect of a floating conductor in a DC field. Lastly, the scope of the dissertation is defined.

2.1 DC field conditions

While HVAC technology has been developed for decades as the standard for power transmission, HVDC technology is relatively new. A fundamental difference between HVDC and HVAC technology is the electric field surrounding the line. While HVAC lines have an oscillating field surrounding it due to the alternating voltage on the line, HVDC transmission lines have a sustained field which is constant in both magnitude and direction.

With HVDC lines, there are three types of configurations, namely monopolar, bipolar and homopolar. With these three types of configurations, the conductors can be at either positive or negative polarity, or a conductor at each polarity as in the case of bipolar lines [8]. This results in transmission lines with a either a constant positive or constant negative electric field. A sustained field at both polarities leads to the interaction of any space charge in the vicinity of the line with this electric field. The presence of space charge in an air-insulated gap is known to distort the field, changing the critical values of breakdown for different geometries [1]. The polarity

of the DC voltage also has an effect on the field distortion due to the behaviour of the space charge in a reversed field when comparing different polarities [1], resulting in an increased number of factors which must be investigated in order to better understand HVDC transmission.

2.2 DC breakdown: streamer and leader mechanisms

The nature of air breakdown under stress from a DC voltage has been reported [9, 10]. Both of these authors observed a transition of corona discharge, to streamer development and finally a leader breakdown. However, the nature of the leader development is not very clear. Suzuki et al. [10] reported a leader developing after the complete traversal of the gap by the initial streamer. Allen et al. [9] on the other hand reported leader development and breakdown before the streamer had traversed the gap. Allen, did note that Suzuki's observations were made under low humidity conditions and suggested that this was the contributory factor towards the difference in their results. Despite this, there was another common result which was that despite an apparent leader mechanism, the mean stress over the gap was similar to that of a streamer gradient, showing the dominance of the streamer mechanism in the breakdown.

It is known that the leader mechanism is initialised by a preliminary streamer mechanism [11, 12]. Bondiou and Gallimberti [12] reported the development of a leader discharge, where it was observed that the leader is initiated by corona in the form of streamer filaments from a common 'stem'. The formation of the leader channel then arises from heating of the stem channel from the flow of streamer current and subsequent detachment of negative ions which ultimately leads to a second phase of corona. The leader then advances with leader corona (in the form of streamers) allowing the leader to propagate into the gap. This means that the predominant mechanism of leader breakdown is still based in streamer breakdown and the advancing space charge that forms the head of streamer. A similar mechanism of leader breakdown is described by Niemeyer et al. [11] where the development and propagation of breakdown in an electronegative gas was considered.

The preliminary streamers and their channels are also discussed in further detail in terms of polarity by Niemeyer et al. [11]. In the the case of postive polarity breakdown, there is a narrow, convergent discharge channel due to the photons and electrons of the proceeding avalanche converging on the head of the streamer,

while in the case of negative polarity breakdown a broad and divergent discharge channel forms due to the photons and electrons from the avalanche moving radially away from the streamer head. Both these polarity-dependant effects are confirmed in preliminary research performed by the author [13] (Also presented in **Appendix C**). In this preliminary research, high-speed photography was used to observe the discharge channels in both positive and negative DC rod-plane gaps. In the case of positive DC breakdown, a narrow and concentrated discharge channel that progresses into the gap was observed, as shown in *Figure 2.1(a)* [13]. In the case of negative DC breakdown, a broad and divergent channel was observed as shown in *Figure 2.1(b)* [13]. These observations clearly demonstrate streamer breakdown that is described by Niemeyer [11] for preliminary streamers, where similar discharge channels are described. This observation also further enforces the idea that although both streamer and leader mechanisms are described for the breakdown of non-uniform gaps under DC stress, the fact that streamer breakdown is provisional to leader development, the breakdown mechanism that can be considered for this research can be restricted to that of a streamer mechanism.

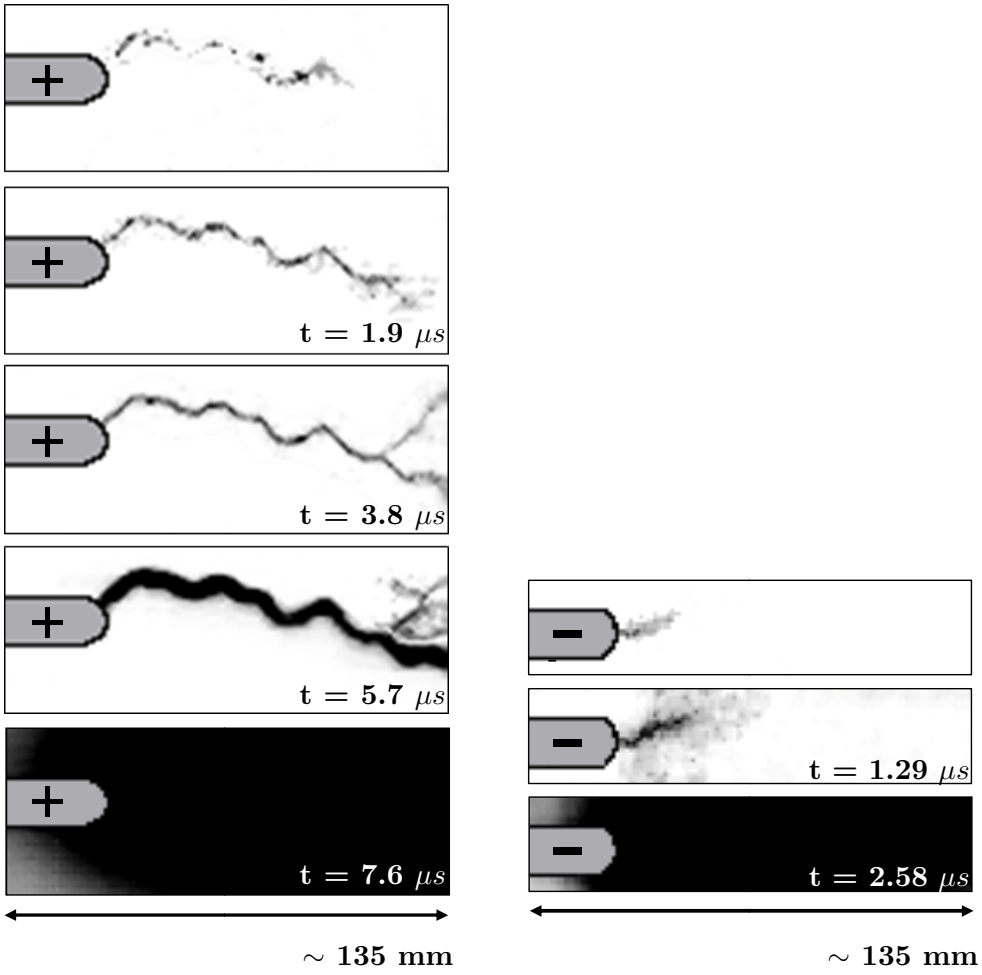
The polarity effect on streamer channels is shown in a sequence of high-speed photographs of the breakdown of a rod-plane gap for both positive and negative polarity in *Figures 2.1(a)* and *2.1(b)* respectively. In Figure *2.1(a)*, there is clearly a defined, narrow channel that propagates into the gap from the energised rod. This is in contrast to the divergent and less-defined channel that propagates under negative DC stress in *Figure 2.1(b)*.

2.3 Previous research

Previous research has been done towards understanding the performance of air insulation under DC stress and on live-line maintenance, however these two topics have been researched in isolation and only with a limited scope in combination.

2.3.1 Live-line maintenance

Previous research on live-line maintenance has focussed on the investigation of switching impulse conditions. Rizk [14], Hutzler [15] and Baldo and Pesavento [16] all modelled the scenario of live-line maintenance using a FC in a non-uniform gap. This successfully models several cases of live-line maintenance, of which involve a worker



(a) *350 mm, positive DC rod-plane gap* (b) *250 mm, negative DC rod-plane gap*

Figure 2.1: High-speed photography of the DC breakdown of a rod-plane gap with a (a) 350 mm gap under positive DC stress and (b) 250 mm gap under negative DC stress

on metal platform, a worker in a conductive suit or an approaching helicopter. In all these cases, a conductor at floating potential is introduced into an air gap between the line and tower geometry.

Hutzler [15] provided a well-rounded investigation into the effect of different geometrical parameters of FCs on the breakdown strength of rod-plane air gaps, showing that a smooth object (i.e. sphere) with a small anodic protrusion has a profound effect on the breakdown strength of a non-uniform gap. This was a more general approach to the effect of FCs on air insulation breakdown strength.

Rizk [14] developed a model to predict the critical switching impulse strength of a gap with air insulation with a large FC present. This model is applicable to investigate live-line maintenance on High Voltage Alternating Current (HVAC) lines with overvoltages, however it does not take into account the effect of a sustained field at either polarity that occurs on HVDC lines.

2.3.2 The breakdown performance of DC gaps

Numerous papers have been published with regard to the performance of air insulation under stress from a DC voltage [10, 17–20]. Menemenlis and Harbec [17] investigated the behaviour of air insulation when stressed by a DC voltage. Feser [18] investigated the effects of humidity on the breakdown voltage of air under a DC voltage. A similar investigation was conducted by Calva et al. [19] whereby the effects of reduced air density at altitude and humidity were both investigated for both polarities of DC voltage. From this research, a detailed investigation was taken at the requirements of correction of DC breakdown voltages to standard conditions, in which polarity dependent correction factors were suggested.

Suzuki et al. [10] investigated the breakdown mechanism of DC flashover for rod-plane gaps which are less than one metre in length. One of the conclusions from his research was that for a positive DC voltage, the breakdown voltage increased linearly with gap spacing, implying a constant gradient. This in contrast to the the case of a negative DC voltage, where the gradient decreases as the gap is increased. Suzuki [10] also suggested that breakdown in the gap progresses from corona discharge to streamer development and lastly leader development.

Allen et al. [20] looked at the breakdown of air insulation under a compositive voltage comprised of a DC voltage and a lightning impulse overvoltage, allowing the effect of a sustained DC field on the breakdown due to switching impulse overvoltages. From the results of this research, the pre-stressing of a rod-plane gap with a negative DC voltage was shown to have a significant effect on the breakdown voltage, where a 25% decrease in the breakdown strength was observed. This is an important observation, as the most onerous case of live-line working is performed when an unpredictable overvoltage occurs on the line. This overvoltage should be a switching impulse as live-line maintenance is not performed during electrical storms [14].

2.3.3 The effect of floating conductors in a DC field

Although the topic of a FC within a DC field has not been extensively researched, there has been previous work into the topic. Research into the effect of FCs on the breakdown performance of DC gaps has been performed by Kubuki et al. [21], however the scope of the research was to investigate the effect of pollution effects using sphere-sphere gaps and sphere-plane gaps. The quasi-uniform test objects used during the research means that it does not extend to a live-line maintenance scenario, where a the non-uniform field geometry is an important physical component. However, the research did investigate the effect of different FC geometries which were shown to have a significant influence on the breakdown strength of the gap. Further research from Kubuki et al. [22] then sought to develop a method to estimate the breakdown voltage of a similar quasi-uniform geometry with a floating needle or a floating sphere within the air gap.

Roman et al. [23] specifically researched the effect of a FC that is close to the ground plane of a quasi-uniform (plate-plate) DC air gap. The effect on the breakdown voltage was shown to be heavily influenced by the charging of the FC due to corona discharge as well as due to the partial breakdown of the air insulation over the secondary gap in the test object.

2.4 Scope of the dissertation

The scope of the dissertation is limited to the construction of a simplified model, numerical analysis of this model in order to predict the effect of a floating conductor in an electric field, and the confirmation of this model with physical experiments in a laboratory. This includes fundamental analysis of the physical breakdown process, when comparing the predicted and measured results.

The size of the air gaps used during the laboratory work was limited by the maximum output of the DC generator in the High Voltage Laboratory (HV Lab) at the University of the Witwatersrand. The maximum output of the generator was limited to 400 kV at both polarities, however this maximum was also reduced due to its use at altitude in Johannesburg. As a result, the size of the non-uniform air gaps used in this research are limited to 0.8 m for positive polarity and 0.25 m for negative polarity. This limitation means that the scope of the research focuses more specifically on the general relationship of a sustained field with a FC and its

effect on streamer breakdown of air insulation.

In the following chapter, the problem addressed in this dissertation is defined with the adopted approach to the research outlined, including a brief overview of the components of the adopted approach.

Chapter 3

Adopted approach

The problem addressed by this dissertation is defined and the adopted approach for the research introduced. A brief overview of the two main components of the research, namely the experimental and research components, is then given.

3.1 Problem statement

Despite live-line maintenance guidelines being implemented for HVAC lines such as by the IEEE [3], and utilities implementing standard practice of HVAC live-line maintenance, specific practices and standards for HVDC lines are not defined. This includes considerations of polarity and reduced air density on air insulation under DC stress during live-line maintenance. With the expected growth of HVDC transmission networks and the necessity of live-line working to aid the delivery of power and reduce stress to these future networks, knowledge of these live-line maintenance scenarios is vital to aid the development of safety guidelines. To provide the foundations of a better understanding of the live-line working scenario on HVDC overhead transmission lines, the effect of a FC on the breakdown strength of non-uniform DC gap is investigated. With the research being conducted at an altitude of 1740 m Above Mean Sea-Level (AMSL), the investigation is specifically of the effect with reduced air density.

3.2 Overall approach taken

The aforementioned research is comprised of two main components:

- **Modelling and simulations**: The scenario of live-line maintenance is modelled with an appropriate test object, consisting of a FC within a rod-plane gap. This test object is then modelled such that its breakdown strength as a function of the position of the FC along the central axis of the gap can be evaluated through simulations. This is achieved by approximating the complex air gap geometries presented by the test object into simple gap geometries (rod-plane gap and rod-rod gap). A numerical prediction of the breakdown of these gaps is then performed in order to estimate the breakdown voltage of the total gap.
- **Laboratory work**: The breakdown strength of a non-uniform, rod-plane gap as a function of the position of a FC along the central axis was investigated.

These components are discussed in more detail in the following sections.

3.3 Modelling and simulations

In order to investigate the effect of a FC on the breakdown strength of non-uniform DC gap, a model was developed that allows an estimation of the breakdown strength of a test object that can then be used in laboratory work to confirm the model. The model is based on the separation of the total gap by the FC into two gaps, namely a primary and secondary gap. The gaps are the simplified into either a rod-rod or rod-plane geometry and their breakdown voltage estimated by numerical calculation based on the results of past research into these simple gap geometries. One of the fundamental aspects of the simulation is based in the calculation of the floating potential of the FC. This is done through Finite-Element Methods (FEM) modelling within the *femm 4.2* software package [24]. The script for the simulation is written in *MATLAB*, with its source code presented in **Appendix B**. Further details about this simulation research component are outlined in **Chapter 4**.

3.4 Laboratory work

Laboratory work was performed in the HV Lab at the University of the Witwatersrand in Johannesburg, South Africa such that the constructed modelled could be critically analysed and the effect of a FC on the breakdown strength of a non-uniform DC gap further understood. The laboratory results are based around the measurement of a breakdown voltage of a non-uniform, rod-plane gap with a FC present within the gap. The position of the FC is varied along the central axis of the rod-plane geometry, and the breakdown voltage for each position recorded from the multimeter on the control panel of the DC generator that was used. At least five measurements were made for each position of the FC, and a U_{50} breakdown voltage obtained as an average of these measured values as per the IEC 606000-1:2010 standard for high voltage testing techniques [25]. The U_{50} breakdown voltage was obtained for both positive and negative polarities of a DC voltage and for two different gap sizes at each polarity. Further details about the laboratory research component are presented in **Chapter 5**.

In the following chapter, the simulation component of the research is discussed in detail. The model used for simulations is presented and discussed. The method for calculating the floating potential of the FC is also discussed along with the method for estimation of breakdown of the model. Lastly, the results from the simulations are presented.

Chapter 4

Modelling and simulations

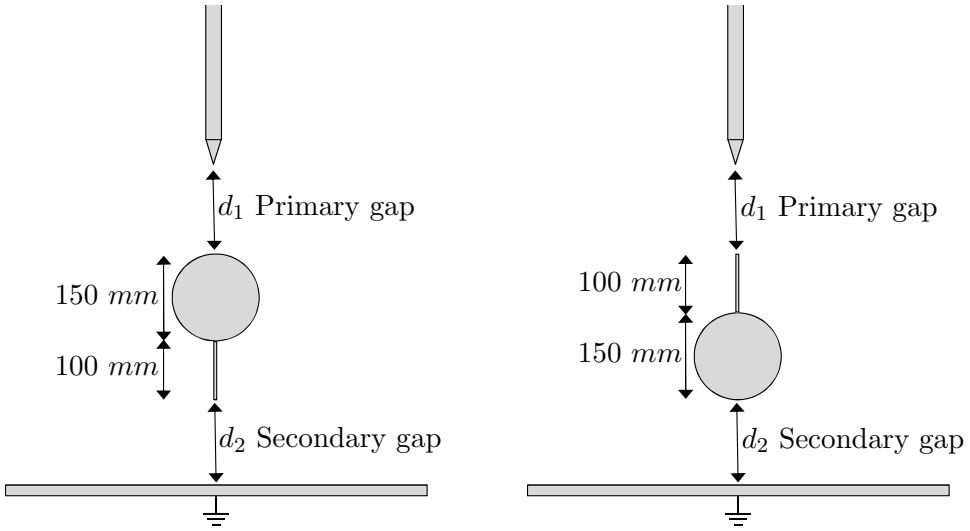
The simulation model is presented and discussed in detail. This discussion includes a look at the capacitive model used for calculating the floating potential of the FC and the method used for estimation of breakdown of the simulation model. Lastly, the results from the simulations are presented.

4.1 Model of the live-line maintenance scenerio

In order to successfully develop a model to be used for simulations, the scenario of live-line maintenance must first be modelled with an appropriate test object. The test object is based on previous research into the case of live-line maintenance for the case of switching impulses, where a FC is inserted into a non-uniform field [2, 14–16]. The non-uniform field is to best represent the nature of the electric field surrounding the conductor of a transmission line. For purposes of simplification, a rod-plane gap is used to generate this field as opposed to a conductor-plane gap or any other non-uniform field geometry. The use of a rod-plane gap as opposed to any other simple non-uniform gap geometry is due to its field also being polarity dependent which is important in the case of DC voltages.

The geometry of the FC is based on past research on floating body potentials and their effect on the breakdown strength of a non-uniform gap [15]. From the conclusions of this work, a sphere with an anodic protrusion was chosen as the FC that would represent the most onerous case of a FC in an electric field. The size of the sphere is based on its availability for the proposed laboratory work, with a sphere with a diameter of 150 mm chosen.

The protrusion chosen to be used in combination with the sphere is a 100 mm diameter square-cut rod with a diameter of 5 mm. The FC was used such that it had an anodic protrusion, as if this is not the case the protrusion does not have any additional effect towards the decay of the breakdown strength of the gap due to the FC [15]. Although, this research did not consider negative polarity, the result was assumed to be consistent for both polarities and so in the case of negative polarity, an inverted FC was employed. The test object with with the FC is shown in *Figures 4.1(a)* and *4.1(b)* for non-inverted (positive polarity) and inverted (negative polarity) FCs respectively.



(a) *Positive polarity* (b) *Negative polarity*

Figure 4.1: Diagram of the test object used to model the live-line working scenario for (a) Positive polarity and (b) Negative polarity

4.2 Simplified gap geometry model

In an effort to predict the effect of the presence and position of a FC in a non-uniform gap the breakdown strength of the test object is predicted through numerical calculation. From *Figures 4.1(a)* and *4.1(b)*, it can be seen that the test object consists of a complex gap, comprised of the primary and secondary gaps which are separated by the FC. This simplified model of a live-line maintenance scenario can then be further simplified into its series components, where the breakdown strength of both gaps are analysed in isolation.

4.2.1 Positive polarity and non-inverted FC

When considering the test object used for positive polarity (with a non-inverted FC), there are effectively two different gap geometries. These are namely a rod-sphere gap and a protrusion-plane gap. However, in order to aid analysis, it is useful to model the two gaps in the form of simple gap geometries. The rod-sphere gap can therefore be viewed as a rod-rod gap (although with two different rod tips and diameters), while the protrusion-plane gap is simply a rod-plane gap. This simplification will allow numerical analysis of the breakdown strength of the gap due to the knowledge of these gap geometries. This model is shown in *Figure 4.2*, clearly showing the assumptions that have been made for the simplification of the gap geometries in the model.

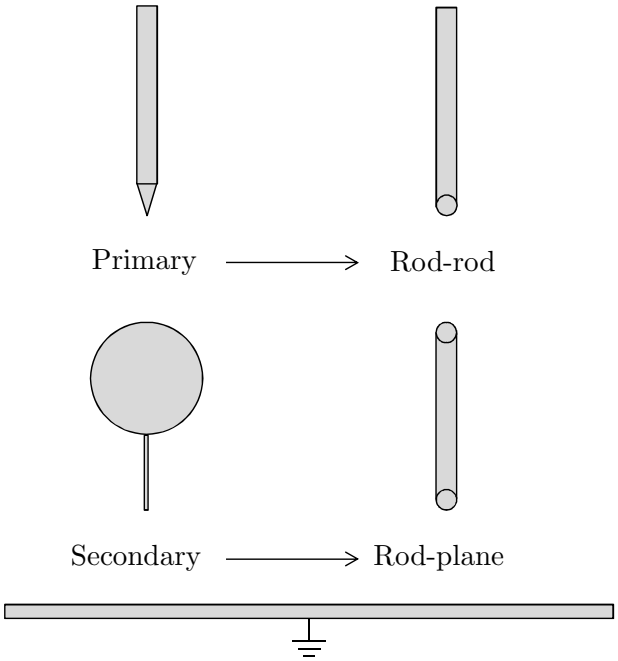


Figure 4.2: The simulation model of the test object for tests with a non-inverted floating conductor

4.2.2 Negative polarity and inverted FC

The negative set-up can be modelled similarly to that of the positive set-up, however the detail lost due to simplification of the gap geometries is different, which should be noted for the interpretation of results arising from use of the model. Firstly, the primary gap in isolation is a rod-protrusion gap, which simply is a rod-rod gap

where the protrusion is now a rod of smaller diameter when compared to the rod. The secondary gap is a sphere-plane gap, and is therefore a simple geometry in its own right. However, as the sphere-plane gap is a mirrored sphere-sphere gap, the gap size that is used in this geometry is more than half the diameter of the sphere itself, thus the geometry abandons the quasi-uniform nature that is assumed when using tables for sphere-sphere gaps. As a consequence of this, the secondary gap is modelled using a rod-plane geometry, whereby the sphere is modelled as a large diameter hemispherical rod. This model is shown in *Figure 4.3*.

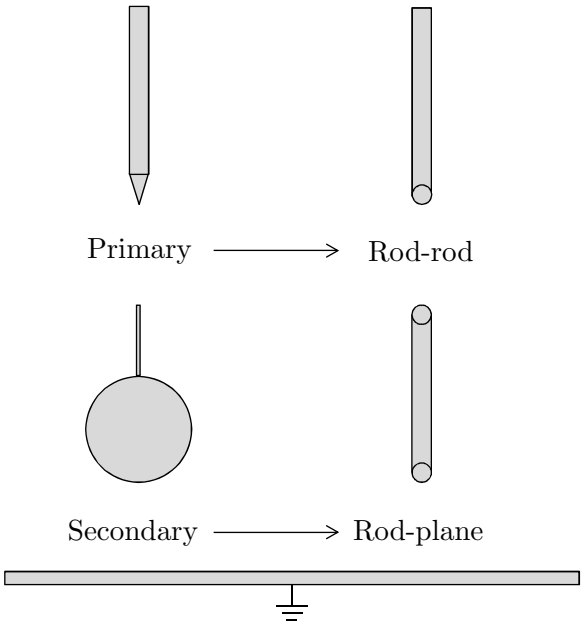


Figure 4.3: The simulation model of the test object for tests with an inverted floating conductor

4.3 Capacitive modelling of the floating potential

In order to be able to perform a numerical calculation of the breakdown strength of the two isolated gaps, the potential of the FC must be known such that the voltage and stress across both the primary and secondary gaps can be known for any geometry. This is achieved by modelling the separate conductors of the test object in terms of their stray capacitances to each other and to infinity, as shown in *Figure 4.4*.

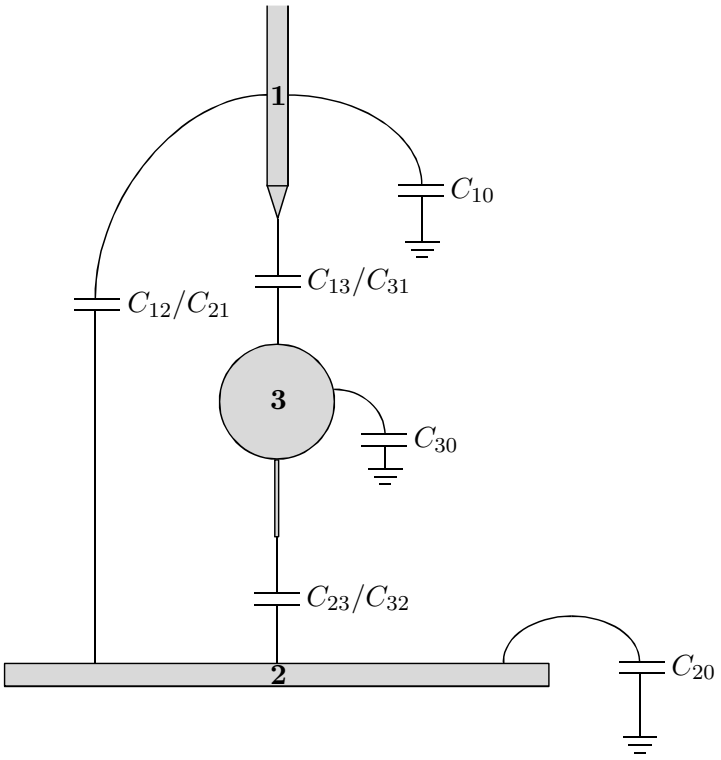


Figure 4.4: The test object in terms of capacitive relationships

A capacitance matrix relates charge to voltage in a given system, with the simple relationship shown in *Equation 4.1* [26].

$$\mathbf{Q} = \mathbf{C} \cdot \mathbf{V} \tag{4.1}$$

where $\mathbf{Q}$ and $\mathbf{V}$ are matrices containing the charge and potential of each conductor respectively, as shown in *Equations 4.2* and *4.3*.

$$\mathbf{Q} = \begin{bmatrix} Q_1 \\ Q_2 \\ \vdots \\ Q_N \end{bmatrix} \tag{4.2}$$

$$\mathbf{V} = \begin{bmatrix} V_1 \\ V_2 \\ \vdots \\ V_N \end{bmatrix} \tag{4.3}$$

The capacitance matrix $\mathbf{C}$ is shown in its general form in *Equation 4.4*, and represents the stray capacitances of each conductor with respect to each other while the diagonal of the matrix represents the self-capacitances of each conductor.

$$\begin{bmatrix} C_{11} & -C_{12} & \cdots & -C_{1N} \\ -C_{21} & C_{22} & \cdots & -C2N \\ \vdots & \vdots & \ddots & \vdots \\ -C_{N1} & -C_{N2} & \cdots & C_{NN} \end{bmatrix} \tag{4.4}$$

The self-capacitances can also be expanded in terms of the stray capacitances represented in *Figure 4.4* and is shown in *Equation 4.5* [26].

$$\begin{bmatrix} C_{10} - C_{12} - \cdots - C_{1N} & & & \\ & C_{20} - C_{21} - \cdots - C_{2N} & & \\ & & \ddots & \\ & & & C_{N0} - C_{N1} - \cdots - C_{N-1} \end{bmatrix} \tag{4.5}$$

When simplifying the model from a generalised model for N conductors, to a more simple three-conductor model that applies to the test object, the capacitive relationship can be represented as in *Equation 4.6*

$$\begin{bmatrix} Q_1 \\ Q_2 \\ Q_3 \end{bmatrix} = \begin{bmatrix} C_{11} & -C_{12} & -C_{13} \\ -C_{21} & C_{22} & -C23 \\ -C_{31} & -C_{32} & C_{33} \end{bmatrix} \begin{bmatrix} V_1 \\ V_2 \\ V_3 \end{bmatrix} \tag{4.6}$$

In the case of calculating the floating potential on the FC, V_1 is set to V which is the applied voltage on the high voltage electrode while V_2 is set to 0 V as it is the grounded plane. The other known quantity is the initial charge on the FC, which is zero prior to any charged particles from ionisation from the high electric field arriving on the FC itself or charging due to corona discharge [26]. This is therefore

just an initial, static case of the test set-up. As a result, Equation 4.6 simplifies to *Equation 4.7*.

$$\begin{bmatrix} Q_1 \\ Q_2 \\ 0 \end{bmatrix} = \begin{bmatrix} C_{11} & -C_{12} & -C_{13} \\ -C_{21} & C_{22} & -C23 \\ -C_{31} & -C_{32} & C_{33} \end{bmatrix} \begin{bmatrix} V \\ 0 \\ V_{FC} \end{bmatrix} \tag{4.7}$$

When solving Equation 4.7, the bottom row becomes

$$0 = -C_{31}V + C_{33}V_{FC} \tag{4.8}$$

When making V_{FC} the subject of the equation, the ratio of the floating potential of the FC to the applied voltage on the rod (V) can given in terms of its self-capacitance (C_{33}) and its mutual capacitance with the energised rod (C_{31}).

$$V_{FC} = kV \tag{4.9}$$

where:

$$k = \frac{C_{31}}{C_{33}} \tag{4.10}$$

The convenience of Equation 4.9 is that the floating potential of the FC can be computed for any geometry, as long as C_{31} and C_{33} can be calculated. In order to calculate these quantities *femm 4.2* is used as a FEM package. If a unit voltage is applied to the FC and 0V is applied to both the rod and plane, the charge on each conductor due to the unit potential on the FC can be computed. Using the capacitive relationship and the fact that the voltage is one, charge and capacitance are equivalent in this case and therefore the capacitance of the FC with respect to the rod and plane, as well as itself, can be calculated.

4.4 Estimation of breakdown

With a simplified model of two isolated gaps and the ability to calculate the potential of the FC, one can now proceed to estimate a critical breakdown voltage of the gap.

This involves firstly calculating the breakdown voltage of the primary gap (V_{b1}) and secondary gap (V_{b2}). As the primary gap is modelled as a rod-rod gap, it can be calculated using Equation 4.11 [1]. This formula is for a rod-rod gap that meets certain specifications such that a rod-rod gap can be used as a measurement device. Although these specifications are not always met by the model, the formula is still used as an approximation.

$$V_{b1} = \delta(A + Bd_1)\sqrt[4]{5.1 \times 10^{-2}(h + 8.65)} \tag{4.11}$$

where:
d_1 is the size of the primary gap
A is 20 kV, B=5.1 kV/cm for positive polarity
A is 15 kV, B=5.45 kV/cm for negative polarity
δ is relative air density
h is absolute humidity (g/m^3)

For calculation of the breakdown voltage of the secondary gap, the estimation of streamer breakdown of a rod-plane gap is used. This uses the streamer gradient of a rod-plane gap to estimate the breakdown strength, whereby a linear relationship between breakdown voltage and gap size is assumed.

$$V_{b2} = E_S d_2 \tag{4.12}$$

where:
E_S is the streamer gradient
d_2 is the size of the secondary gap

The streamer gradient is polarity dependent and is obtained from a consolidation of past research presented by Allen and Boutlendj [27], where the mean streamer gradient for breakdown for positive polarity rod-plane gaps is approximately 500 $kV.m^{-1}$. The streamer gradient for negative polarity is less documented, however based on the mean stress for negative DC breakdown reported in further work by Allen et al. [9] a value of approximately $1200kV.m^1$ is used.

The breakdown voltage of both gaps can now be calculated and from this a critical

value of the applied DC voltage (V_{HV}) can be found which will cause the breakdown of both gaps. V_{b1} gives the potential across the primary gap and relates to the potential of the FC (V_{FC}) and the applied DC voltage (V_{FC}) as follows.

$$V_{b1} = V_{HV} - V_{FC} \tag{4.13}$$

Using Equation 4.9 and making V_{HV} the subject of the equation leads to a direct equation relating the applied DC voltage to V_{b1}, shown in Equation 4.14.

$$V_{HV} = \frac{V_{b1}}{1 - k} \tag{4.14}$$

Now the algorithm depicted in *Figure 4.5* on the following page can be used to determine the critical value of V_{HV} that will cause complete breakdown of the complex gap.

An assumption used for the algorithm is that V_{HV} is at a value such that it will just cause breakdown of the primary gap when calculated using Equation 4.14. V_{FC} is then computed and the behaviour of the secondary gap is predicted from relating the value of V_{b2} to V_{HV} and V_{FC}. This algorithm is then repeated for increments of the primary gap size, with the position of the FC varied from touching the rod until touching the plane. The script used in $MATLAB$ is presented in **Appendix B**.

4.4.1 Assumptions and limitations of the model and simulations

From *Figures 4.2* and *4.3* earlier in the chapter, it can be seen that both test set-ups are effectively modelled by the same geometries, with a resulting rod-plane gap with a rod as the FC. However, for interpretation of the simulation results against physical results from laboratory work, the actual test object and the differences that arise in the simplified geometry of both the primary and secondary gaps must be considered. This is important as the choice of a sphere with protrusion was based on work by Hutzler [15] that also considered a rod as the FC and found that it had less of an effect on the breakdown strength than a sphere with anodic protrusion.

Furthermore, the way that the floating potential of the FC is computed assumes a certain initial condition that the FC has a nett charge of zero. However, when ionisation of air through corona discharge takes place there is a presence of charged

1: **Input:** $d, d_0, d_1, polarity$
2: **Output:** $V_{bd}, case_{bd}$
3: $d_2 \Leftarrow d - d0 - d1$ ▷ determine length of secondary gap

$\boxed{A}$ *Primary gap*

4: ***if*** *polarity = 1* ***then*** ▷ $\therefore$ *positive polarity*
5: $A = 20kV$, $B = 5.1kV.cm^{-1}$, $E_S = 500kV.m^{-1}$
6: ***else*** ▷ $\therefore$ *negative polarity*
7: $A = 15kV$, $B = 5.45kV.cm^{-1}$, $E_S = 1100kV.m^{-1}$
8: ***end if***
9: $V_{bd1} \leftarrow (A + Bd_1)\sqrt[4]{5.1 \times 10^{-2}(8.65 + 11)}$ ▷ *Breakdown voltage of the primary, rod-rod gap*

$\boxed{B}$ *Secondary gap*

10: $V_{b2} \leftarrow E_s d_2$ ▷ *Breakdown voltage of the secondary, rod-plane gap*

$\boxed{C}$ *Floating potential of the FC*

11: $k \leftarrow \frac{C_{31}}{C_{33}}$ ▷ C_{31} *and* C_{33} *determined using FEM in femm 4.2*

$\boxed{D}$ *The instant just before breakdown of the primary gap*

12: $V_{HV} \leftarrow \frac{V_{b1}}{1-k}$
13: $V_{FC} \leftarrow kV_{HV}$ ▷ *Floating potential of the FC*
14: ***if*** $V_{b2} < V_{FC}$ ***then*** ▷ *Check breadown strength of secondary gap*
15: $V_{HV} \leftarrow \frac{V_{b2}}{k}$ ▷ *As secondary gap breaks down, the FC is effectively earthed*
16: ***if*** $V_{HV} \leq V_{b1}$ ***then***
17: $V_{bd} = V_{b1}$ ▷ *As the FC is earthed,* V_b1 *is sufficient for complete breakdown*
18: ***else***
19: $V_{bd} = V_{HV}$ ▷ *Breakdown occurs as the FC is earthed*
20: ***end if*** ▷ *Partial breakdown of secondary gap prior to complete breakdown*
21: ▷ *Breakdown depends on primary gap*
22: ***else if*** $V_{b2} \geq V_{FC}$ & $V_{b2} \leq V_{HV}$ ***then***
23: $V_{bd} = V_{HV}$ ▷ *Sequential breakdown of the primary and then secondary gap*
24: ▷ *Breakdown depends on primary gap*
25: ***else if*** $V_{b2} > V_{HV}$ ***then***
26: $V_{bd} = V_{b2}$ ▷ *Partial breakdown of the primary gap prior to complete breakdown*
27: ▷ *Breakdown depends on secondary gap*
28: ***end if***

Figure 4.5: The algorithm used for prediction of the breakdown voltage of the rod-plane gap with a floating conductor

particles in a sustained electric field. This aspect of the problem is omitted from the model as it uses an electrostatic solution.

4.5 Simulation results

The aforementioned simulations were done for two cases:

- Positive polarity, non-inverted FC
- Negative polarity, inverted FC

In both cases, the larger of the two gap sizes are was used for simulations. The estimated breakdown voltages of the both the positive and negative polarity simulations is shown as a function of the position of the FC in *Figures 4.6* and *4.7* respectively at the end of the chapter. The position of the FC is identified by the ratio (in percentage form) of the primary gap to the total series gap. *Tables 4.1* and *4.2* summarise the position nomenclature in terms of both ratio and actual primary gap size in the test set-ups simulated for positive and negative polarity respectively.

In the following chapter, the laboratory component of the research is discussed in detail. This includes an overview of the testing facility, laboratory set-up in the laboratory as well as the general methodology. Lastly, the results from the laboratory work are also presented.

Table 4.1: Position nomenclature for the positive polarity test set-up

Primary gap d_1 (mm)	**Secondary gap d_2 (mm)**	**FC position**
100	700	12.5%
200	600	25%
300	500	37.5%
400	400	50%
500	300	62.5%
600	200	75%
700	100	87.5%

Table 4.2: Position nomenclature for the negative polarity test set-up

Primary gap d_1 (mm)	**Secondary gap d_2 (mm)**	**FC position**
31.25	218.75	12.5%
62.5	187.5	25%
93.75	156.2	37.5%
125	125	50%
156.25	93.75	62.5%
187.5	62.5	75%
218.75	31.25	87.5%

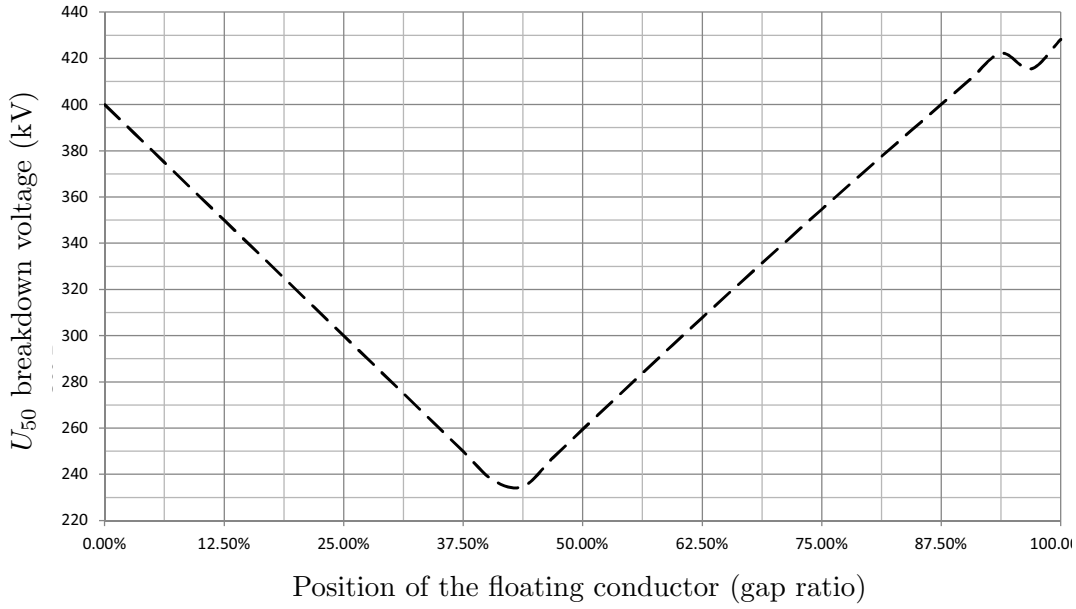


Figure 4.6: Predicted breakdown strength of a positive DC gap with floating conductor as a function of the position of the floating conductor

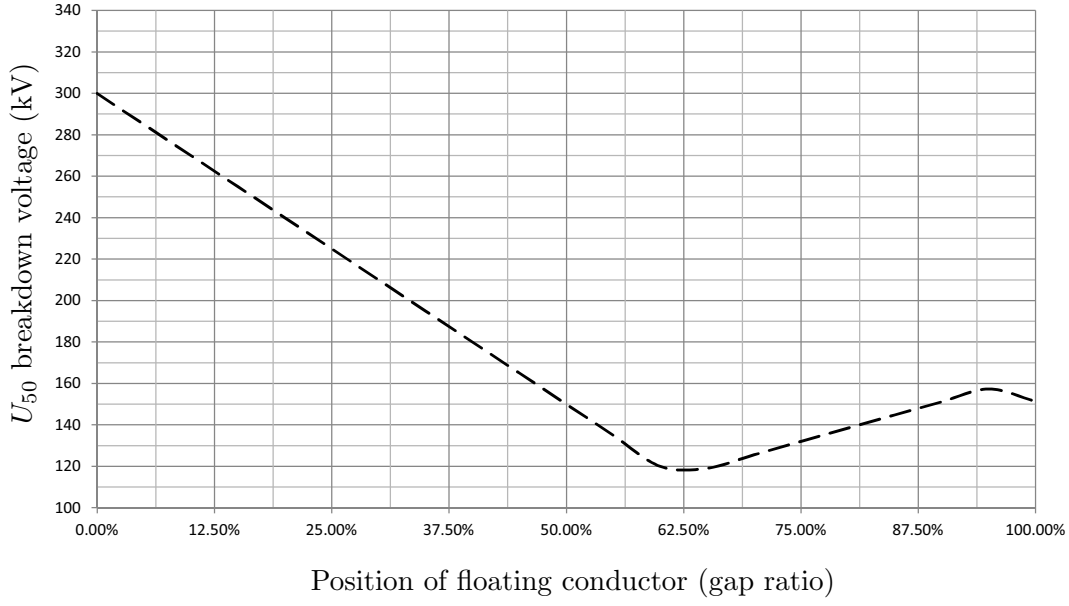


Figure 4.7: Predicted breakdown strength of a negative DC gap with floating conductor as a function of the position of the floating conductor

Chapter 5

Laboratory work

The different aspects of the laboratory work are presented and discussed. A description of the testing facility (High Voltage Laboratory at the University of the Witwatersrand) is given. An outline of the laboratory set-up and the methodology adopted for the laboratory work is shown before the results of the laboratory component are presented. These results present the change in the breakdown voltage of the test gap as the FC is moved from close to the rod, towards the plane.

5.1 Testing facility

Laboratory work was conducted in the HV Lab at the University of the Witwatersrand in Johannesburg, South Africa. The location of the laboratory means that all experiments were conducted at an altitude of 1740 m, allowing for the effects of the FC to be assessed for a reduced pressure and air density scenario. During testing, environmental conditions (temperature, pressure and relative humidity) were recorded such that the results can be corrected for standard conditions. The recorded environmental conditions are contained in **Appendix A**. Taking into account the environmental conditions and using the complete application of correction factors for each experiment as specified in the IEC 606000-1:2010 standard [25], the results presented in this chapter are for standard environmental conditions. The calculated correction factors for the different sets of results is also included in **Appendix A**.

5.2 Laboratory set-up

The laboratory set-up consists of the following main components:

- DC Generator
- Rod-plane test gap
- Floating conductor

A photograph of the test set-up in the HV Lab at the University of the Witwatersrand is shown in *Figure 5.1*, with the test set-up in position for a positive DC test with the FC at the 50% position.



Figure 5.1: Photograph of the test set-up used during laboratory work in the HV Lab at the the University of the Witwatersrand

5.2.1 Generator

The generator used was a 400 kV DC generator, rated at 15 mA maximum output current. However, due to the laboratory work being conducted in Johannesburg at an altitude of 1740 m above sea level, the actual output of the generator was further restricted to approximately 320 kV. When the generator was raised above

this voltage, flashover would occur on the circuit of the generator itself (as pictured in *Figure 5.2*).



Figure 5.2: Still from a video of flashover over the circuit of the DC generator in the HV Lab at the University of the Witwatersrand

5.2.2 Rod-plane test gap

The main test gap used during all laboratory work was a rod-plane gap, in order to produce a non-uniform field with a standard geometry. The rod-plane gap consisted of the following components:

- 0.5 m long, 16 mm diameter rod with a 30° conical tip
- 1.2 m × 2.0 m steel sheet (2 mm thick)
- 1.5 m Bakelite insulator

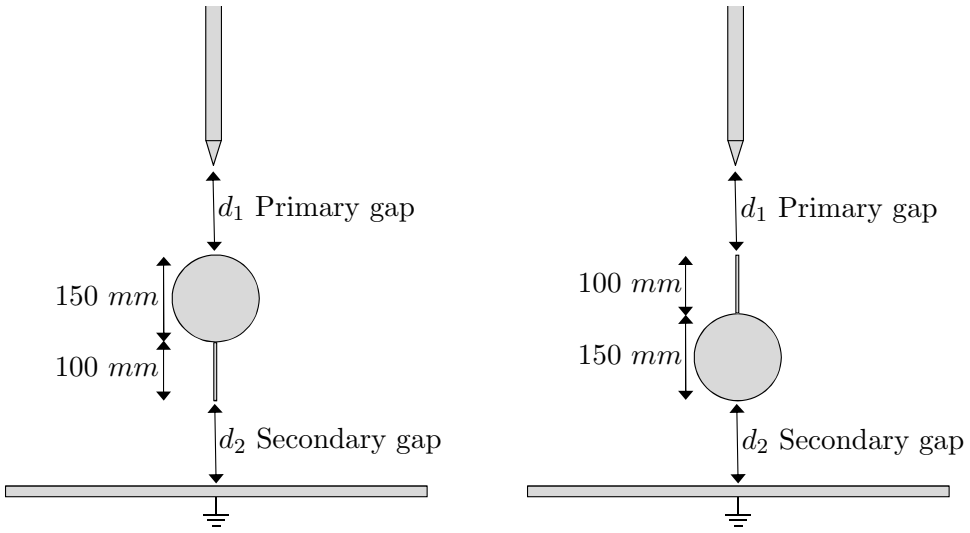
The Bakelite insulator was hung from a motorised crane that runs across the ceiling of the HV Lab. This crane allowed for the position and height of the rod to be varied according to the specifications of the experiment, while the insulator ensured

that flashover did not occur between the energised rod and the crane itself. The steel sheet was located on top of a table and was earthed.

5.2.3 Floating conductor

As previously mentioned in **Chapter 4**, a FC is inserted into a non-uniform field to model the scenario of live-line maintenance. For all laboratory work, a 150 mm diameter copper sphere with a 100 mm protrusion was employed. The geometrical specifications of the sphere are based on past research on floating body potentials and their effect on the breakdown strength of a non-uniform gap [15]. From the conclusions of this work, a sphere with an anodic protrusion was chosen as the FC that would represent the most onerous case.

The protrusion is a 5 mm diameter square-cut rod. The FC was orientated such that it had an anodic protrusion, as if this is not the case the protrusion does not have any additional effect towards the decay of the breakdown strength of the gap [15]. The test-setup with with the FC is shown in *Figures 5.3(a)* and *5.3(b)* for non-inverted (positive polarity) and inverted (negative polarity) FCs respectively.



(a) *Positive polarity* (b) *Negative polarity*

Figure 5.3: Diagram of the test set-up used for laboratory work with (a) Positive polarity and (b) Negative polarity

5.3 Methodology

The laboratory work consisted of two main components with tests involving positive and negative polarity. However, the basic test procedure for both set-ups was similar and is shown in in *Figure 5.4*. The main test procedure was based on the determination of the U_{50} breakdown voltage of a rod-plane gap for different positions of the FC within the gap. The U_{50} breakdown voltage was determined using the IEC 606000-1:2010 standard [25], with an applied DC voltage being linearly increased (ramped) until breakdown occurred and the breakdown voltage being noted. This is repeated at least five times for each specific set-up, with the average value giving the U_{50} breakdown voltage.

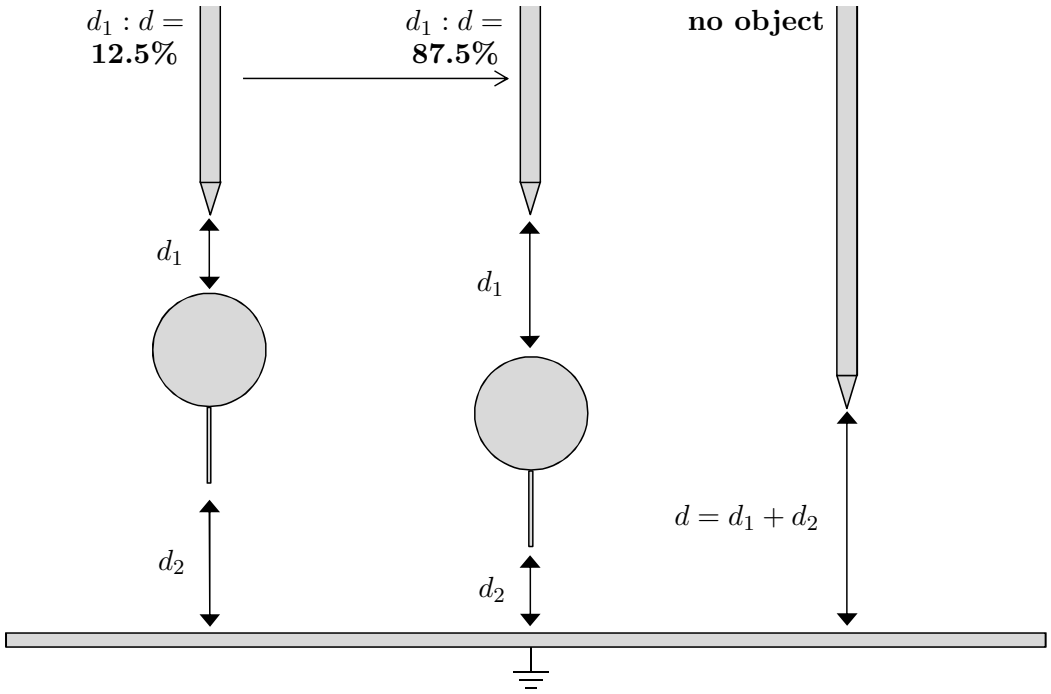


Figure 5.4: The laboratory procedure during the laboratory work

The presence of a FC within the test object means that the object must be earthed after every application of a shot in order to discharge any floating charge on the object. The physical reasons for this is due to the FC becoming charged when there is a discharge from the FC to earth [23]. This fact was observed when earthing the FC as a small discharge was observed between it and the earth stick. No specific waiting period was observed for reparation of the air insulation, based on the fact that residual ions will not have an effect on the breakdown voltage as pre-breakdown

ionisation occurs throughout the experiment in the form of corona discharge.

In order to keep a consistent ramp rate for the applied DC voltage, a rate of approximately 3 $kV.s^{-1}$ was used by calibrating the fine control on the variac connected to the transformer of the generator. As the ramp rate for the U_{50} test with an applied DC voltage is not explicitly specified, the choice of a ramp rate of 3 $kV.s^{-1}$ is based on a trade-off of accuracy and time in terms of performing the laboratory work. While a sufficient accuracy of all laboratory work is desired, preliminary work in the laboratory did not show any significant increase in accuracy when decreasing the ramp rate from 3 $kV.s^{-1}$, while the time to perform the laboratory would increase linearly.

5.4 Laboratory results

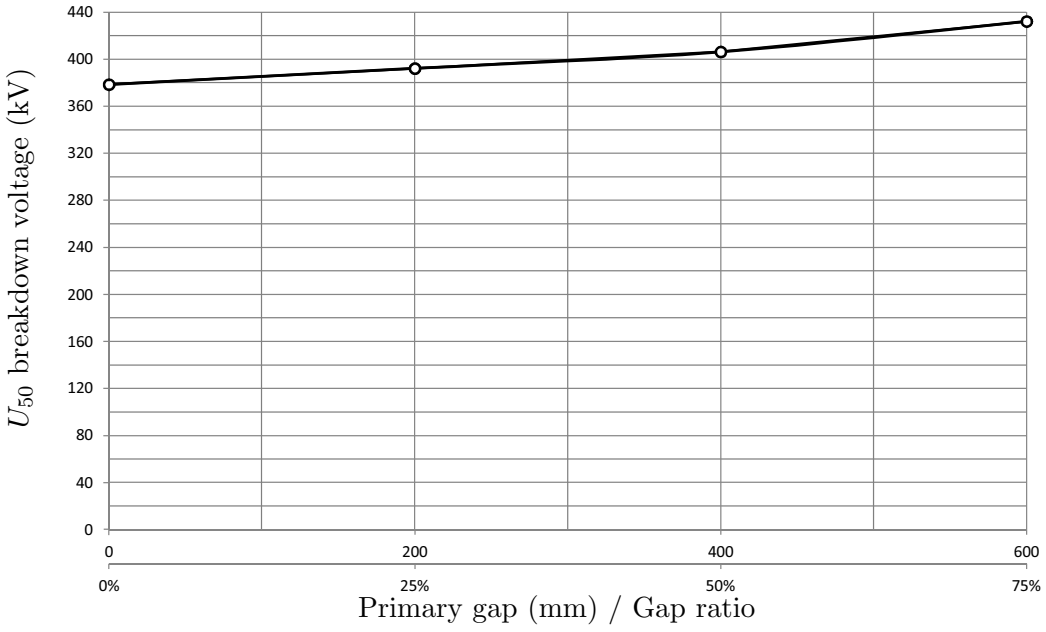
The U_{50} breakdown voltage (corrected for standard environmental conditions) as a function of the primary gap length for both gap sizes of the positive polarity work is presented in *Figure 5.5* on the following page. Only four data points are present for the positive DC gap experiments, namely 0% to 75% in 25% increments.

The results for the negative polarity work (also corrected for standard environmental conditions) for both gap sizes are presented in *Figure 5.6* at the end of the chapter. The base case, where a rod-plane gap with size equal to the total gap size, is represented by the 0% position in the results. This is done so that the base case and results versus the positon of the FC can be presented on the same set of axes.

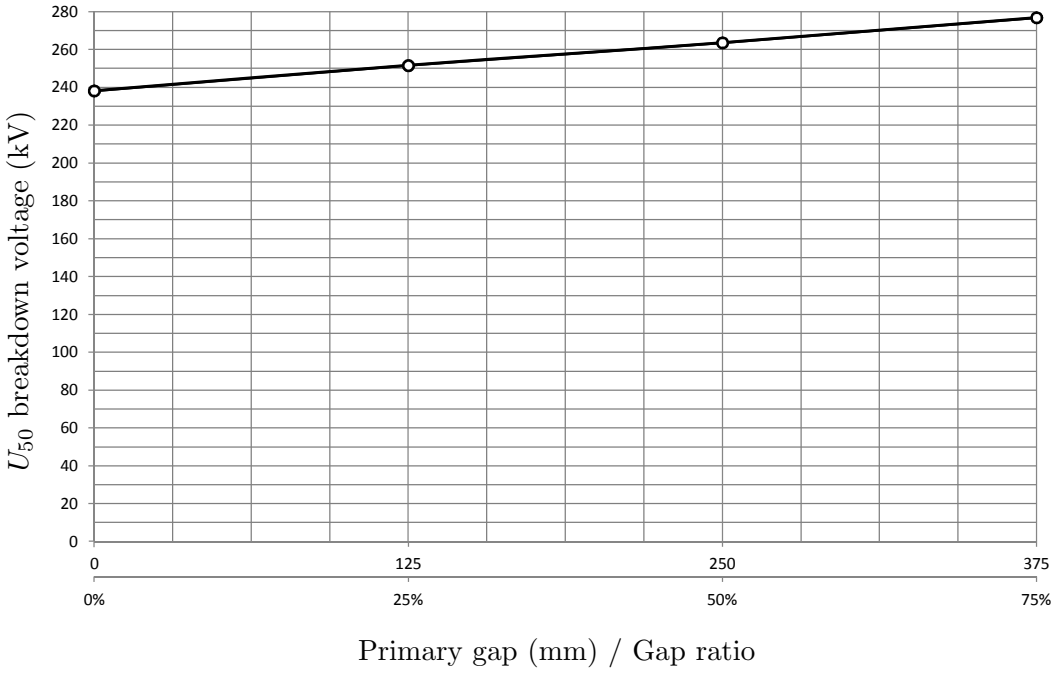
Additionally, in *Figure 5.6(a)*, there are additional data points that relate to the occurrence of two U_{50} breakdown levels at the 37.5%, 62.5% and 82.5% positions of the FC. These correspond to a higher and lower breakdown level, while the actual U_{50} plot in *Figure 5.6(a)* uses a mean of all the breakdown voltages at each position.

These results will be discussed in detail in **Chapter 6**, where they can be viewed in conjunction with the simulation results from **Chapter 4** in order to critically analyse the developed model and simulations.

In the following chapter, the results from both the laboratory and simulation components are analysed and discussed, both in isolation and comparatively. The possible reasons for discrepancies between the laboratory and simulation results are introduced and critically analysed.

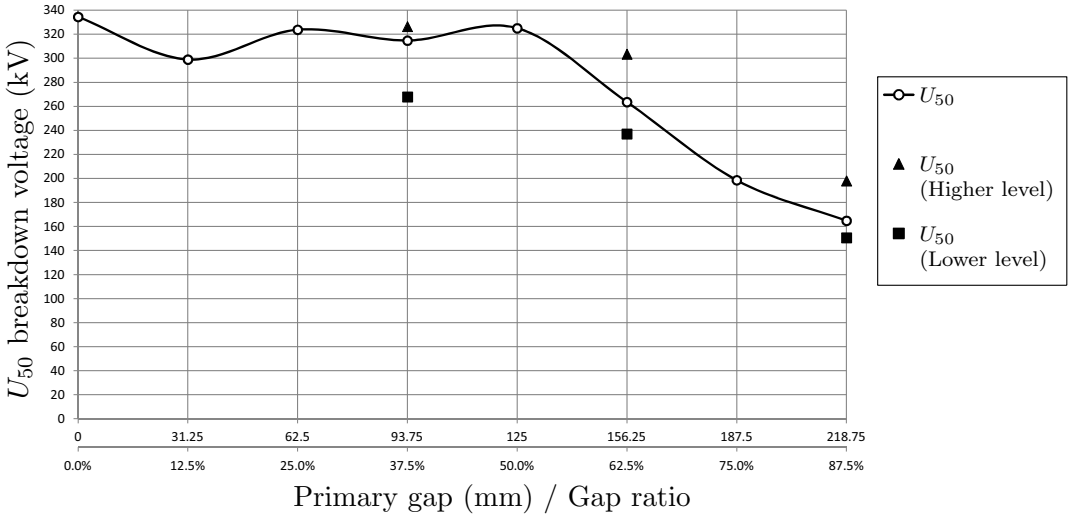


(a) $d_1 + d_2 = 80$ *cm*

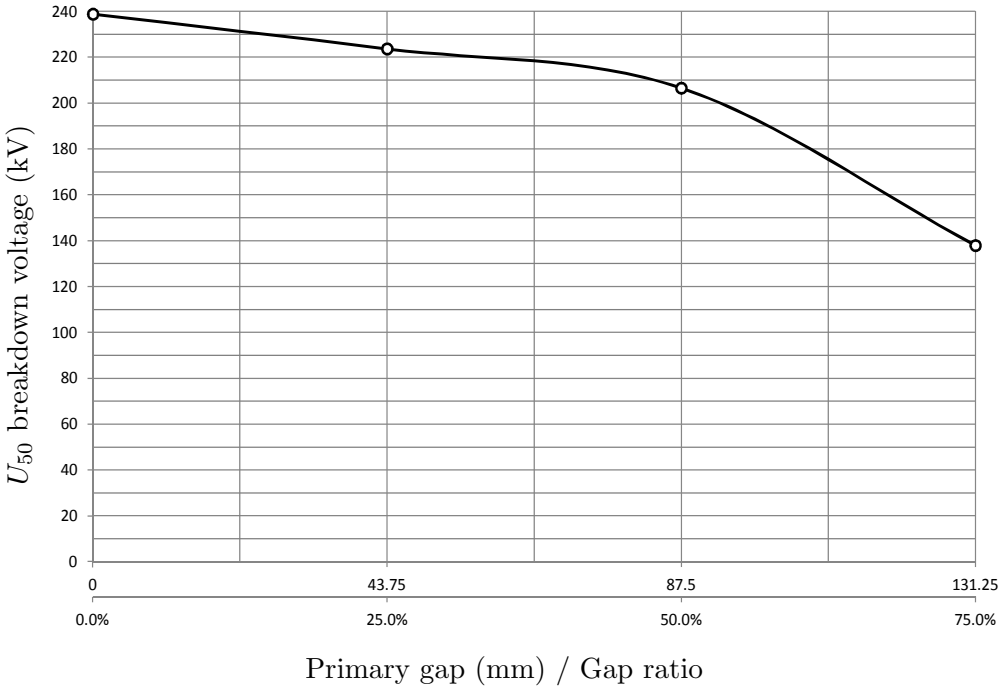


(b) $d_1 + d_2 = 50$ *cm)*

Figure 5.5: U_{50} breakdown voltage (corrected for standard environmental conditions) of a positive DC rod-plane gap with a floating conductor with (a) $d_1 + d_2 = 80$ cm and (b) $d_1 + d_2 = 50$ cm



(a) $d_1 + d_2 = 25$ cm



(b) $d_1 + d_2 = 17.5$ cm

Figure 5.6: U_{50} breakdown voltage (corrected for standard environmental conditions) of a negative DC rod-plane gap with an inverted floating conductor with (a) $d_1 + d_2 = 25$ cm and (b) $d_1 + d_2 = 17.5$ cm

Chapter 6

Analysis and discussion

The results from both the laboratory and simulation components of the research are analysed in detail. This analysis includes looking at both sets of results in isolation as well as a comparative analysis in order to critically analyse the developed model. Discrepancies between the two sets of results are critically assessed with possible reasons for these arising problems presented and discussed.

6.1 Overview of the laboratory results

The laboratory work is split into two parts which will be analysed in isolation. They are the following:

- Positive DC with a non-inverted FC
- Negative DC with an inverted FC

Furthermore, each part of the laboratory work consists of two different gap sizes in order to obtain a more general view of the effect of the FC on the breakdown strength of the test gap.

The laboratory results in brief show that:

- The introduction of a FC into a positive DC rod-plane gap, increases the strength of the gap when compared to a gap size equal to the total complex gap size.

- The positive DC breakdown strength increases as the FC is moved from the energised conductor.
- The introduction of a FC into a negative DC rod-plane gap decreases the strength of the gap when compared to a the base case of a rod-plane gap with a total gap that is equivalent to the split gap size.
- With a FC present, the negative DC breakdown strength has a maximum value close to the 50% position of the object and minimum value as the FC approaches the ground plane.
- The effect of the FC on the breakdown strength for both polarities is outlined in *Table 6.1*, with the maximum observed change from the no-object case presented.

Table 6.1: The maximum change in the breakdown strength of the DC test gaps with the introduction of a floating conductor

Polarity	**Gap size (mm)**	**Breakdown strength change (%)**
Positive	500	16.2 (at 75% position)
	800	14.2 (at 75% position)
Negative	175	-42.2 (at 75% position)
	250	-40.6 (at 75% position) / -50.7 (at 87.5% position)

6.1.1 Positive polarity

The effect of a FC on a rod-plane gap energised by a positive DC voltage is presented in *Figure 6.1.* As can be seen in *Figure 6.1*, the breakdown voltage increases as the primary gap increases, and this result is consistent for both gap sizes. When interpreting this result, it means that the further the FC moves away from the energised electrode, the higher the breakdown strength of the gap. The percentage increase in the primary gap strength is similar for both gap sizes too, with a 16.2% and 14.2% increase in the breakdown strength at the 75% position for the 80 cm and 50 cm gaps respectively.

This result suggests that the most critical point of the FC in a positive DC non-uniform field is close to the conductor. However this result must be taken in context, as the gap sizes for which tests were conducted were limited by the maximum output of the DC generator, with gap sizes that are less than one metre used.

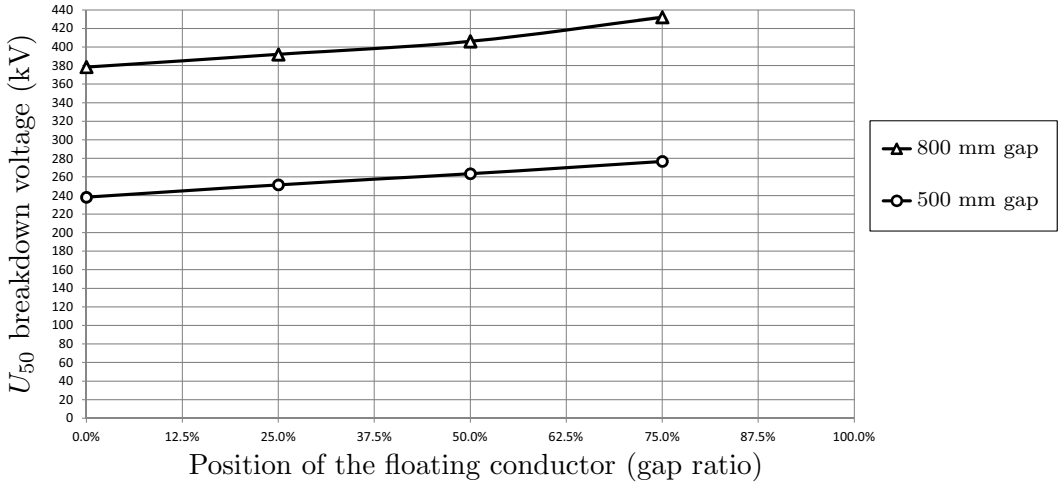


Figure 6.1: Overview of the positive polarity results for both test gap sizes

6.1.2 Negative polarity

Figure 6.2 shows the effect of the position of the FC on the breakdown strength of a rod-plane gap energised by a negative DC voltage when the FC is inverted. From *Figure 6.2*, a decline is observed in the breakdown strength of both test gaps as the FC approaches the ground plane. Unlike in the positive case, the breakdown strength of the negative DC gap is immediately lowered by the presence of the FC within the gap regardless of its position. Another notable difference in the effect of the FC in the negative case is that of the severity in the change of the breakdown strength. In the case of a 250 mm total gap size, the breakdown strength reduced by 50.7% when the FC was at the 82.5% position. Comparatively, the change of the breakdown strength in the positive case in the most onerous result is 16.2% with the FC at the 75% position.

In *Figure 6.2*, the breakdown strength of a 250 mm gap changes sporadically prior to the major decline of the breakdown strength of the gap after the 50% position of the FC. The reason for this is not clear, however it may be accounted to a small degree of movement of both the rod and the charged FC within the sustained electric field as the field intensity increases close to breakdown.

Another observation from the negative DC laboratory work is that three positions in the 250 mm tests (37.5%, 62.5% and 82.5%) had results which showed two distinct levels in the U_{50} test, from an increased total of ten shots, as is shown in *Figure 5.6(a)*. A similar observation was made by Baldo and Pesavento [16], where they observed two distributions of values for breakdown probability. Their

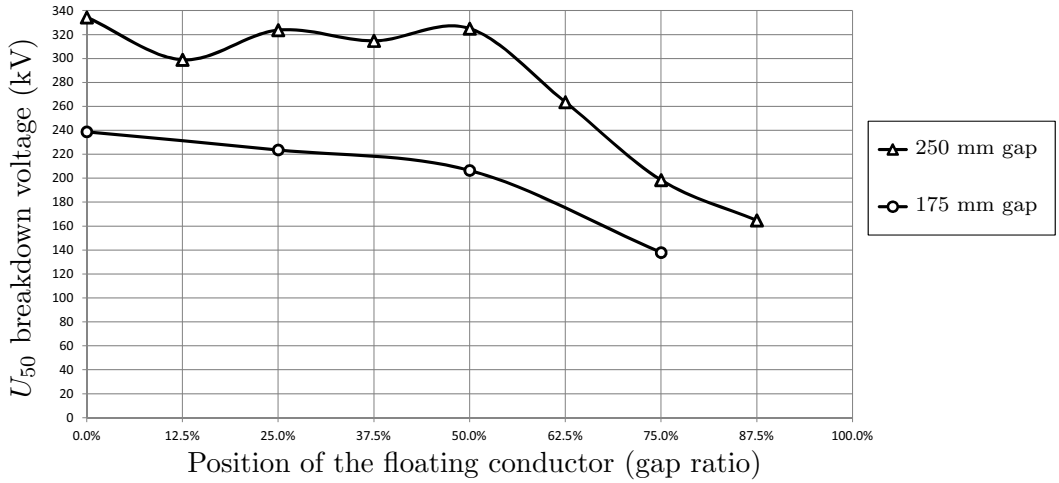


Figure 6.2: Overview of the negative polarity results for both test gap sizes

set-up consisted of a sphere-plane gap with a floating plate. The range between the two levels was always present, however the two distributions became more distinct as length and capacitance of the secondary gap changed, with an increase in the definition of the distributions as the secondary gap was increased and the capacitance of the gap decreased.

During these specific parts of the laboratory work, the level at which breakdown occurred was highly dependent on the observed corona. In the case of the lower U_{50} level, intense corona would occur prior to breakdown with visible streamers and hissing occurring. In the case of the higher U_{50} voltage, this observed corona would stop short (with very little visible corona in comparison) and then breakdown would occur at a much higher voltage, as shown in *Table 6.2*. At the 82.5% positon, where the conductor was closer to the plane, when breakdown occurred multiple subsequent breakdowns would occur just after the initial breakdown. The different values for the U_{50} breakdown voltage in these instances are presented for comparative purposes in *Table 6.2* along with the number of breakdowns at each level.

These observations suggest that the interaction of charged particles from corona discharge in the sustained DC field has a very strong influence on the breakdown strength of a negative DC gap. Additionally, there is also the factor of negative ions and electrons formed from corona discharge arriving on the FC and changing the charge of the FC. This presents an electrostatic problem which is actually transient in nature.

Table 6.2: Number of breakdowns at each level for the case of two distinct U_{50} levels in three negative polarity tests

FC position	Level	Breakdown voltage (kV)	No. of breakdowns
37.5%	Mean	314.7	10
	Lower	267.8	2
	Higher	326.4	8
62.5%	Mean	263.6	10
	Lower	237.0	6
	Higher	303.5	4
82.5%	Mean	164.8	10
	Lower	150.6	7
	Higher	198.0	3

6.2 Overview of simulation results and the model

The effect on the breakdown strength of the gap can be explained by the fact that the introduction of the FC has effectively changed the geometry of the gap. With the separation of the gap into two gaps, namely a primary and secondary gap, it has also introduced polarity dependent effects regarding the breakdown strength of the two gaps.

The fact that a positive DC gap appears to increase in breakdown strength with the introduction of a FC relates to the introduction of a quasi-symmetrical geometry into the test object in the form of a rod-rod gap. This rod-rod gap is in the form of a rod-protrusion gap in the negative polarity case, and in the form of a sphere-rod gap in the positive polarity case.

The simulations take into account this change in geometry and use it to calculate the breakdown strength of both the primary and secondary gap in isolation. However, the results from these simulations have discrepancies when compared to the results from the laboratory results. To demonstrate this, in the case of positive polarity, *Figure 6.3* shows that simulations predict an initial decline in the breakdown strength as the FC is moved from the HV rod until the FC is at approximately the 40% position, after which there is a sharp rise in the breakdown strength as the FC approaches the ground plane. This is in comparison to a gradual rise in the breakdown strength of the set-up in laboratory results. It is also apparent that the change in the breakdown voltage from the starting to the ending points, the

simulation and laboratory results have a good agreement with each other. This is shown with a predicted 7.06% increase in the breakdown voltage from the starting (0%) to ending (100%) position of the FC in the simulation results, compared to an increase of 14.2% when at the 75% position in the laboratory results. This suggests that there is some omitted detail in the model that is present when both the primary and secondary gaps are of significant size in relation to each other. This result for the starting and ending points is also consistent in the case of negative polarity.

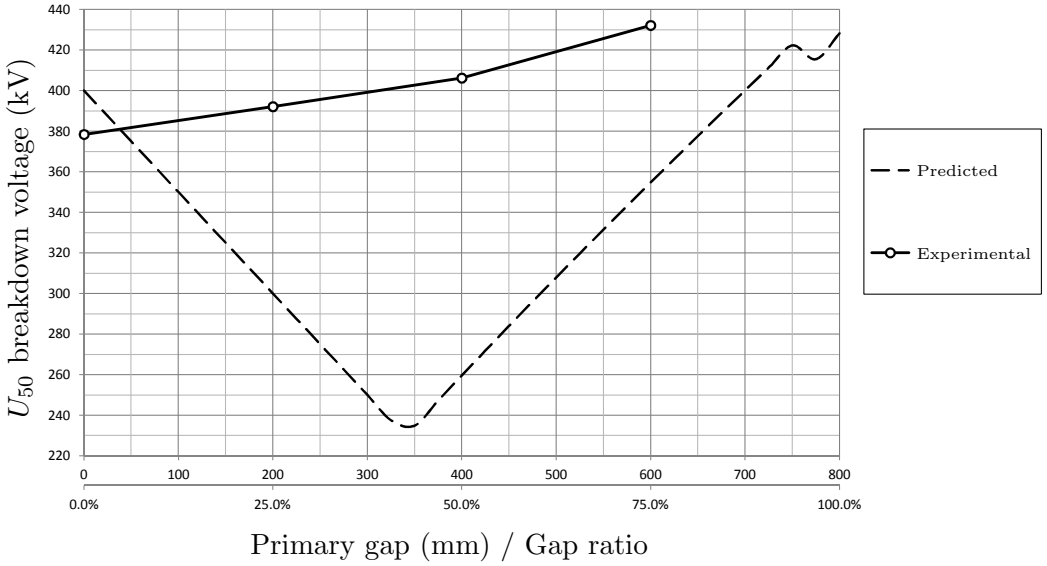


Figure 6.3: Predicted and observed breakdown strength of a positive DC gap with a floating conductor as a function of the position of the floating conductor

In the case of negative polarity, *Figure 6.4* shows that the predicted trend is for the breakdown strength of the gap to decrease as the FC is moved towards the ground plane. This agrees with the laboratory results, although there are slight discrepancies. While the predicted results show a sharp but steady decline in the breakdown strength up until the 70% position, laboratory results show a sporadic change in the breakdown strength up until the 50% position of the FC, before a severe decline in the breakdown strength as it further approaches the grounded plane. The predicted results also show a minor recovery of the breakdown strength from the 70 % position of the FC, which is absent in the laboratory results. As with the positive case and mentioned earlier, there is also agreement between the laboratory and predicted results at the starting and ending points. This is shown with a predicted 49.6% decrease in the breakdown voltage from the 0% to 100% position of the FC in the simulation results, while a decrease of 50.7% in the breakdown voltage was

observed at the 82.5% position in the laboratory results.

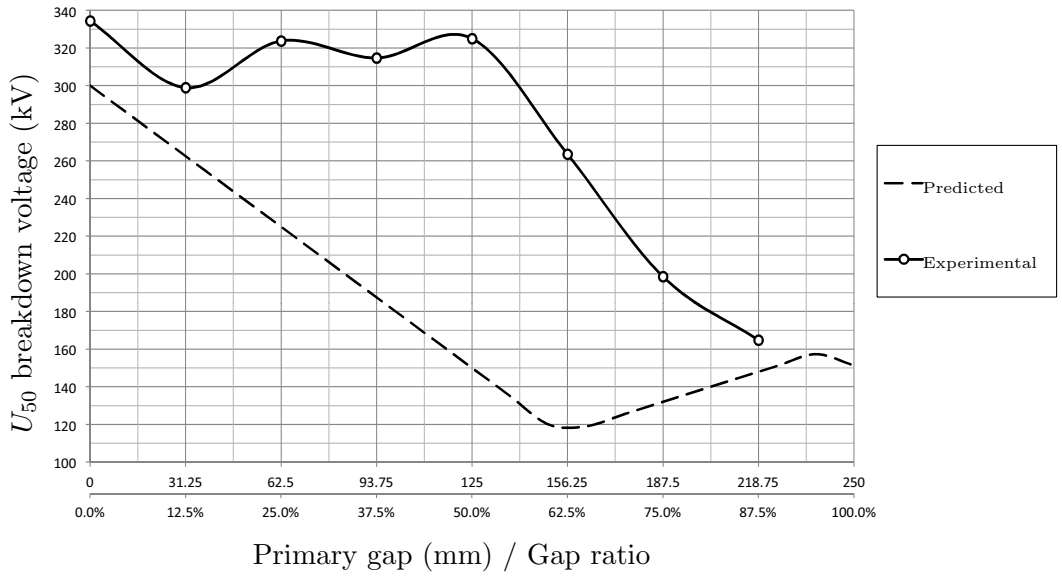


Figure 6.4: Predicted and observed breakdown strength of a negative DC gap with a floating conductor as a function of the position of the floating conductor

From this comparison between laboratory and simulation results, it is apparent that the model developed for simulation work has omitted detail which results in the observed discrepancies between the simulation and laboratory results. The shortcomings of the model will be explored in the following section.

6.3 Shortcomings of the model

An explanation towards the differences in the simulation and laboratory results will be explored in terms of omitted detail and shortcomings of the model. The following details will be analysed for both polarities:

- Additional parameters affecting the floating potential
- Over-simplification of the geometry
- Absent effect of corona and pre-breakdown discharges
- The lack of dynamic electrostatic scenario

6.3.1 Additional parameters affecting the floating potential

In the model used for simulations, the floating potential of the FC was calculated exclusively from the induced potential from the high voltage rod due its geometrical position and the electrostatic relationship of the FC to the rest of the test object geometry. However, the potential of the FC is made up of three components, and can be expressed as shown in Equation 6.1 [14].

$$V_{FC} = V_g + V_i + V_c \tag{6.1}$$

where:
V_g is the potential due to the geometry
V_i is the induced potential due to space charge
V_c is the potential due to accumulated charge on the surface of the FC

Within the simulation model, only V_g has been accounted for. In previous work by Rizk [14], it was shown that considering the potential due to accumulated charge may have a notable effect on the breakdown voltage on a complex gap. Its also feasible to assume that due to the large surface area of the sphere component of the FC in relation to the diameter of the rod, a large amount of charge may accumulate on the surface of the FC. However, any accumulated charge on the FC should be significantly reduced by corona discharge due to the presence of an anodic protrusion [15].

The second component of the potential of the FC which was ignored is the induced potential due to space charge. This component is difficult to predict due to the inability to easily quantify the space charge in the test set-up. However, the test set-up is under a sustained DC field and thus the interaction of any free charge arising from corona discharge could be an important factor, resulting in a significant component of the floating potential which was omitted.

6.3.2 Geometry simplification

Another explanation for the difference in laboratory and simulation results can be accounted to the geometrical differences in the model when compared to the actual test set-up. When analysing the simplification of the primary gap to a rod-rod gap,

it is clear that the diameter of the sphere and its approximation as a rod will result in an altered field distribution to that expected in a rod-rod gap.

This difference can be analysed in terms of a field efficiency factor (η) which relates the maximum field (E_{max}) to the mean field (E_{mean}) in a certain geometry [1]. It is described by the relationship

$$\eta = E_{max}/E_{mean} \tag{6.2}$$

In results documented in [1] for a 100 mm rod-plane gap for a positive DC voltage, η increases as the diameter of the rod is increased. The value of η corresponding to a selection of relevant rod diameters from these results is shown in *Table 6.3*. Also presented in *Table 6.3* is the change in breakdown voltage as η changes.

Table 6.3: Approximate decline of the breakdown strength of a positive DC rod-plane gap (100 mm) as a function of rod diameter and the field efficiency factor [1]

Rod diameter (mm)	η (%)	**Breakdown voltage (kV)**
10	5	100
25	15	50
50	25	75
100	40	150
250	60	200
∞	100	266

From *Table 6.3*, it is evident that as the diameter of the rod increases, η too increases. Although this is a result for a rod-plane gap, this result is intuitive and should be applicable to a rod-rod gap as one would expect a less non-uniform field as the diameter of one rod increases. Another trend from the results is that as η increases so does the breakdown voltage of the gap, except for very small values of η where pre-discharges and space charge alter the field distribution [1]. This effect of non-uniformity is also present with negative DC voltages, but the critical values of η are different [1].

When applying this to our simplified model, it is clear that the sphere, with a diameter of 150 mm will have a much higher field efficiency factor than that presumed for a simple rod-rod gap (in positive polarity) or a rod-plane gap (in the negative polarity case) which will change the breakdown voltage of the respective gaps, and

consequently the breakdown voltage of the entire complex gap. The predicted effect of the gap geometries containing the sphere would therefore be to increase the breakdown voltage relative to that which is calculated with the sphere simplified to a rod.

It is also clear that the protrusion, with a diameter of 5 mm will have a much smaller field efficiency factor and will similarly change the breakdown voltages calculated with the simplified geometries. The effect of the protrusion and its resulting field efficiency factor is more complex due to the aforementioned effect of pre-discharges and space charge in the gap. This aspect of the test set-up will be analysed in more detail in the following subsection.

6.3.3 Absent effect of corona and pre-breakdown discharges

It was observed in **Section 6.1** that corona discharge can have a significant effect on the mechanism of breakdown in a gap with a FC in it, with it leading to two separate but distinct U_{50} breakdown levels. As corona would be a large source of charged particles (electrons and ions) [28], their interaction in the field at a critical point in the gap (one of the effective electrodes of the both the primary and secondary gaps in the form of the FC) would seem to have a significant effect on the effective breakdown of the gap.

The presence of a FC in a rod-plane air gap has many consequences. Firstly, it effectively short-circuits the air insulation over its entire length, reducing the air gap. It then also changes the geometry of the non-uniform gap, introducing polarity dependant effects. Part of the change in geometry is the introduction of high curvature points within the gap, especially around the protrusion of the FC. This protrusion acts as a corona source [15] and so as the voltage across the gap is increased, so does the electric stress around it and thus corona discharge occurs. There has been significant research performed into the role of corona discharge on the breakdown strength of air gaps by Feser [29] and Roman et al. [23].

Feser [29] researched and documented the influence of corona discharge on both rod-plane and rod-rod gaps. He concluded that the breakdown voltage of these gaps was not only influenced by space charge but also by the products of the corona discharge that then remain in the gap.

This general observation can be backed up by a more in-depth analysis of the physics

of corona discharge from a FC [23]. Taking the positive set-up with the non-inverted FC, corona inception will take place on the protrusion of the FC in the form of positive corona. This corona will charge the FC negatively, thus reducing the field in the secondary gap and enhancing the field in the primary gap. From the simulation results in *Figure 6.3*, the breakdown strength of the secondary gap determines the breakdown strength of the complex gap for $d1 : \ 0\% \ \rightarrow \ 50\%$, this reduction of electric field in the secondary gap, would lead to a larger required breakdown voltage.

6.3.4 The lack of dynamic electrostatic scenario

From the aforementioned details of the model that may account for the difference in laboratory results from the predicted results of the simulation work, there is one predominant detail that results in an incomplete model. This is the fact that the simulations only consider a static scenario. The actuality of the laboratory work is that there is a vast amount of change in the physical scenario, as charged particles are produced by corona and these particles are accelerated and moved through the ever-increasing intensity of a sustained DC electric field as the voltage is increased. The result is that the simulation model is in fact a static model of a dynamic problem. The result therefore only considers a snapshot of the test set-up when the FC has a charge of zero and there are no charged particles within the gap. This condition will only be valid at the beginning of the experiment before any corona pre-discharge and ionisation of air has occurred. With the corona discharge that was observed during the laboratory work, this condition would not be for the majority of the experiment during which intense visible and audible corona was observed throughout.

The absence of a model for the build-up and movement of space charge in the air insulation means that the presented simulation model does not accurately model the effect of a FC on the breakdown strength of a DC gap. The start and end points in *Figures 6.3* and *6.4* show agreement between the simulation and laboratory results, which suggests that the model is accurate when the FC is close to the energised rod or grounded plane.

Chapter 7

Conclusions and recommendations

Recommendations for future research is suggested such that improvements and progress can be made on the current work. Conclusions from the conducted research are then summarised.

7.1 Recommendations

The provisional nature of the conducted research means that there is a broad area for building on the results of this dissertation. Firstly, the research only considered breakdown of an air gap from stress by a DC voltage. Considering the case of HVDC live-line maintenance, the most onerous case which must be considered is that in which a switching overvoltage occurs on a HVDC line, and there is effectively a composite voltage comprised of a impulse superimposed on a DC voltage. Therefore the presented research should be modified such that the effect of a FC on the breakdown of a pre-stressed DC gap with a superimposed switching impulse is investigated. This case would give a more realistic scenario of live-line maintenance and paint a clearer picture of the effects of a FC in the most onerous case.

In addition, attempted high-speed photography failed to capture the breakdown mechanism when a FC was present in the gap. This was a result of insufficient luminosity of the pre-breakdown events. However with appropriate peripheral equipment, such as a photomultiplier, these pre-breakdown mechanisms can be captured and analysed in conjunction with any physical results. It should also be noted that if research with a composite voltage is attempted, the energy and luminosity of pre-breakdown mechanisms will be considerably higher which may allow the effective use of high-speed photography even in the absence of a photomultiplier.

The suspected role of space charge and corona discharge on the breakdown strength of a gap with a sustained field from a DC voltage can be investigated further. The envisaged research which is recommended is a dynamic measurement of the electric field at critical points in the gap geometry as the applied voltage is increased. These critical points could be at either side of the FC and at the rod and plane, allowing the progression of space charge in the gap to be measured.

Lastly, this research was specifically conducted for the case of reduced air density, with the laboratory located at 1740 m above sea-level in Johannesburg. All the results have been corrected for standard conditions of temperature, pressure and humidity as per the IEC 60060-1 standard, however to fully understand the effect of a FC on the breakdown strength of a DC gap, the research should be confirmed at sea-level.

7.2 Conclusion

From the results and analysis that have been presented in this dissertation, the following conclusions can be made:

1. The predicted breakdown from simulation results and laboratory results are vastly different, however the model still gives a correct general trend when the FC is either close to the rod or plane. The differences in these results are accounted to omitted detail in the model such as:
    - A more complex source of the floating potential of the FC
    - The effect of corona discharge on the potential across each gap due to the change in the nett charge of the FC.
    - The effect of a sustained field from an HVDC source on space charge resulting from corona, and its interaction in the field at critical points in the gap, such as at the FC itself.
    - Deviation of the test geometry from a simple rod-rod and rod-plane gap and, as a consequence, the change in the degree of non-uniformity in the gap in comparison to the model.
    - The absence of a dynamic model which looks at the change in the electrostatic scenario as the applied voltage is increased towards the breakdown voltage.

2. The presence of a FC in a non-uniform air gap has a notable effect on the DC breakdown strength of the gap. This effect is polarity dependent, with an increased breakdown strength in the case of a positive voltage and a decreased strength in the case of a negative voltage. As the FC is moved towards the ground plane, this effect is enhanced with an increasing breakdown strength for positive DC voltages and a decreasing breakdown strength for negative DC voltages.

3. The sensitivity of the breakdown strength to the presence of corona discharge was observed, with the laboratory results showing two distinct U_{50} levels for the results of the U_{50} breakdown voltage of a negative DC gap with the FC at three out of the six positions. The presence of two distinct U_{50} levels is accounted to the strong connection between breakdown strength and corona discharge in a DC field. This conclusion is based on the distinct differences in the corona prior to breakdown between the cases of breakdown at the different levels.

References

[1] E. Kuffel, W. Zaengl, and J. Kuffel, *High Voltage Engineering: Fundamentals*, 2nd ed. Newnes, 2000.

[2] Task Force 07.02 of CIGRE Study Committee 33: Britten, Fonseca, Garbagnati, Hutzler, Zheng-Jianchao, "Strength of external insulation during live line maintenance and repair work with special reference to transient overvoltages," *Electra*, vol. 129, pp. 108–131, March 1990.

[3] "IEEE guide for maintenance methods on energized power lines," *IEEE Std 516-2009*, pp. 1 – 143, 24 2009.

[4] A. Britten, L. Pillay, P. Naidoo, F. Bologna, D. Muftic, and N. Ijumba, "Eskom's proposed strategic research into HVDC transmission," Energize, July 2005.

[5] E. F. Raynham, *Apollo - Cahora Bassa: Enigma and Diversions.* EE Publishers, 2004.

[6] Enhanced access to electricity for Southern Africa - the Caprivi Interconnector. European Commision. Last accesed: 3 May 2012. [Online]. Available: http://ec.europa.eu/europeaid/what/energy/sustainable/cs_caprivi_en.htm

[7] Eskom, "Transmission ten year development plan: 2012 - 2021," 2011.

[8] N. Ijumba and G. Sibilant, *The planning, design and construction of overhead powerlines.* Crown Publications cc, Feb 2005, ch. 4, pp. 68–92.

[9] N. Allen, M. Boutlendj, R. Hughes, H. Lightfoot, and R. Neville, "Analysis and comparison of rod-plane and rod-rod gaps as direct voltage measurement devices," *Science, Measurement and Technology, IEE Proceedings A*, vol. 139, no. 6, pp. 279 – 284, Nov 1992.

[10] T. Suzuki, K. Miyake, and T. Hara, "Breakdown process in rod-to-plane gaps with dc voltages," *IEEE Transactions on Industry Applications*, vol. IA-21, no. 1, pp. 26– 34, 1985.

[11] L. Niemeyer, L. Ullrich, and N. Wiegart, "The mechanism of leader breakdown in electronegative gases," *IEEE Transactions on Electrical Insulation Vol. 24 No. 2, April 1989*, vol. 24, no. 2, pp. 309 – 324, April 1989.

[12] A. Bondiou and I. Gallimberti, "Theoretical modelling of the development of the positive spark in long gaps," *J. Phys. D: Appl. Phys.*, vol. 27, pp. 1252 – 1266, 1994.

[13] C. Hart, K. Nixon, and I. Jandrell, "Initial research into quantifying the effect of a sustained DC field on breakdown phenomena using high-speed photography," in *Proceedings for the 17th International Symposium on High Voltage Engineering*, 2011.

[14] F. Rizk, "Effect of floating conducting objects on critical switching impulse breakdown of air insulation," in *IEEE Transactions on Power Delivery*, vol. 10, no. 3, July 1995, pp. 1360–1370.

[15] B. Hutzler, "Switching impulse strength of air gaps containing a metallic body at floating potential," in *Fifth International Symposium on High Voltage Engineering*, 1987.

[16] G. Baldo and G. Pesavento, "Floating potential bodies and discharge characteristics," in *Seventh International Symposium on High Voltage Engineering*, 1991.

[17] C. Menemenlis and G. Harbec, "Behavior of air insulating gaps of dc systems under impulse, dc and composite voltages," *Power Apparatus and Systems, IEEE Transactions on*, vol. PAS-98, no. 6, pp. 2065 –2075, Nov 1979.

[18] K. Feser, "The influence of humidity on the breakdown voltage of d.c. and a.c. voltages in air," *Bulletin ASE*, vol. 63, no. 6, pp. 278 – 281, 1972.

[19] P. Calva, V. del Moral, M. Marquez, and G. Cabrera, "New proposal of correction factors for dc voltages," in *Electrical Insulation and Dielectric Phenomena, 2003. Annual Report. Conference on*, Oct 2003, pp. 455 – 458.

[20] N. Allen, C. Huang, K. Cornick, and D. Greaves, "Sparkover in the rod-plane gap under combined direct and impulse voltages," *Science, Measurement and Technology, IEE Proceedings* -, vol. 145, no. 5, pp. 207 –214, Sept 1998.

[21] M. Kubuki, R. Yoshimoto, K. Tanoue, and M. Hara, "Breakdown characteristics in air gaps with artifical floating metals under dc voltage," *IEEE Transactions on Dielectrics and Electrical Insulation*, vol. 2, no. 1, pp. 155 – 165, Feb 1995.

[22] M. Kubuki, R. Yoshimoto, K. Yoshizumi, S. Tsuru, and M. Hara, "Estimation of dc breakdown mechanisms in air gaps containing floating metallic particles," *Dielectrics and Electrical Insulation, IEEE Transactions on*, vol. 4, no. 1, pp. 92 –101, Feb 1997.

[23] F. Roman, V. Cooray, and V. Scuka, "Corona from floating electrodes," *Journal of Electrostatics*, vol. 37, no. 12, pp. 67 – 78, 1996.

[24] D. Meeker, "Finite Element Method Magnetics, Version 4.2 (11Apr2012 Build)," http://www.femm.info.

[25] "High voltage test techniques - Part 1: General definitions and test requirements," *IEC 60060-1*, 2010.

[26] W. Fu, S. Ho, S. Niu, and J. Zhu, "Comparison study of finite element methods to deal with floating conductors in electric field," *Magnetics, IEEE Transactions on*, vol. 48, no. 2, pp. 351 –354, Feb 2012.

[27] N. Allen and M. Boutlendj, "Study of the electric fields required for streamer propagation in humid air," in *Science, Measurement and Technology, IEE Proceedings A*, vol. 138, no. 1, 1991.

[28] P. S. Maruvada, *P. Sarma Maruvada*, third edition ed., ser. EPRI AC Transmission Line Reference Book200 kV and Above. Electric Power Research Institute, 2005, ch. 8, pp. 1–40.

[29] K. Feser, "Influence of corona discharges on the breakdown voltage of air gaps," *Proc. IEE*, vol. 118, no. 9, pp. 1309 – 1313, Sept 1971.

Bibliography

- Enhanced access to electricity for Southern Africa - the Caprivi Interconnector. Last accesed: 3 May 2012.
- Fastcam SA5 Hardware Manual (Revision 1.00E). Photron Limited, May 2009.
- IEEE guide for maintenance methods on energized power lines. *IEEE Std 516-2009*, pages 1 – 143, 24 2009.
- High voltage test techniques - Part 1: General definitions and test requirements. *IEC 60060-1*, 2010.
- N.L. Allen and M. Boutlendj. Study of the electric fields required for streamer propagation in humid air. In *Science, Measurement and Technology, IEE Proceedings A*, volume 138, 1991.
- N.L. Allen, M. Boutlendj, R.C. Hughes, H.A. Lightfoot, and R.B. Neville. Analysis and comparison of rod-plane and rod-rod gaps as direct voltage measurement devices. *Science, Measurement and Technology, IEE Proceedings A*, 139(6):279 – 284, Nov 1992.
- N.L. Allen, C.F. Huang, K.J. Cornick, and D.A. Greaves. Sparkover in the rod-plane gap under combined direct and impulse voltages. *Science, Measurement and Technology, IEE Proceedings* -, 145(5):207 –214, Sept 1998.
- G. Baldo and G. Pesavento. Floating potential bodies and discharge characteristics. In *Seventh International Symposium on High Voltage Engineering*, 1991.
- E M Bazelyan, Yu P Raizer, and N L Aleksandrov. The effect of reduced air density on streamer-to-leader transition and on properties of long positive leader. *J. Phys. D: Appl. Phys.*, 40:4133 – 4144, 2007.
- A Bondiou and I Gallimberti. Theoretical modelling of the development of the positive spark in long gaps. *J. Phys. D: Appl. Phys.*, 27:1252 – 1266, 1994.
- A.C. Britten, Logan Pillay, Pat Naidoo, F.F. Bologna, D Muftic, and Nelson Ijumba. Eskom's proposed strategic research into HVDC transmission. Energize, July 2005.
- P.A. Calva, V. del Moral, M.G. Marquez, and G.P. Cabrera. New proposal of correction factors for dc voltages. In *Electrical Insulation and Dielectric Phenomena, 2003. Annual Report. Conference on*, pages 455 – 458, Oct 2003.

- G. Carrara and L. Thione. Switching surge strength of large air gaps: A physical approach. *Power Apparatus and Systems, IEEE Transactions on*, 95(2):512 – 524, mar 1976.
- Eskom. Transmission ten year development plan: 2012 - 2021, 2011.
- K. Feser. Influence of corona discharges on the breakdown voltage of air gaps. *Proc. IEE*, 118(9):1309 – 1313, Sept 1971.
- K. Feser. The influence of humidity on the breakdown voltage of d.c. and a.c. voltages in air. *Bulletin ASE*, 63(6):278 – 281, 1972.
- K Feser and H Singer. From the glow corona into the breakdown. *ETZ-A*, 93:36 – 39, 1972.
- W.N. Fu, S.L. Ho, Shuangxia Niu, and Jianguo Zhu. Comparison study of finite element methods to deal with floating conductors in electric field. *Magnetics, IEEE Transactions on*, 48(2):351 –354, Feb 2012.
- C.L. Hart, K.J. Nixon, and I.R. Jandrell. Initial research into quantifying the effect of a sustained DC field on breakdown phenomena using high-speed photography. In *Proceedings for the 17th International Symposium on High Voltage Engineering*, 2011.
- B. Hutzler. Switching impulse strength of air gaps containing a metallic body at floating potential. In *Fifth International Symposium on High Voltage Engineering*, 1987.
- Nelson Ijumba and Gary Sibilant. *The planning, design and construction of overhead powerlines*, chapter 4, pages 68–92. Crown Publications cc, Feb 2005.
- B. Jones and R.T. Waters. Air insulation at large spacings. In *Proceedings of the Institution of Electrical Engineers*, volume 125, pages 1152– 1176, 1978.
- A. Konrad and M. Graovac. The finite element modeling of conductors and floating potentials. *Magnetics, IEEE Transactions on*, 32(5):4329 –4331, sep 1996.
- M. Kubuki, R. Yoshimoto, K. Yoshizumi, S. Tsuru, and M. Hara. Estimation of dc breakdown mechanisms in air gaps containing floating metallic particles. *Dielectrics and Electrical Insulation, IEEE Transactions on*, 4(1):92 –101, Feb 1997.
- Mamoru Kubuki, Ryuichi Yoshimoto, Kazuki Tanoue, and Masanori Hara. Breakdown characteristics in air gaps with artifical floating metals under dc voltage. *IEEE Transactions on Dielectrics and Electrical Insulation*, 2(1):155 – 165, Feb 1995.
- E. Kuffel, W.S. Zaengl, and J. Kuffel. *High Voltage Engineering: Fundamentals*. Newnes, 2nd edition, 2000.

- P. Sarma Maruvada. *P. Sarma Maruvada*, chapter 8, pages 1–40. EPRI AC Transmission Line Reference Book200 kV and Above. Electric Power Research Institute, third edition edition, 2005.
- D.C. Meeker. Finite Element Method Magnetics, Version 4.2 (11Apr2012 Build). http://www.femm.info.
- C. Menemenlis and G. Harbec. Behavior of air insulating gaps of dc systems under impulse, dc and composite voltages. *Power Apparatus and Systems, IEEE Transactions on*, PAS-98(6):2065 –2075, Nov 1979.
- L. Niemeyer, L. Ullrich, and N. Wiegart. The mechanism of leader breakdown in electronegative gases. *IEEE Transactions on Electrical Insulation Vol. 24 No. 2, April 1989*, 24(2):309 – 324, April 1989.
- Eustace F. Raynham. *Apollo - Cahora Bassa: Enigma and Diversions.* EE Publishers, 2004.
- F.A.M. Rizk. A model for switching impulse leader inception and breakdown of long air-gaps. *Power Delivery, IEEE Transactions on*, 4(1):596 –606, jan 1989.
- Farouk Rizk. Effect of floating conducting objects on critical switching impulse breakdown of air insulation. In *IEEE Transactions on Power Delivery*, volume 10, pages 1360–1370, July 1995.
- Francisco Roman, Vernon Cooray, and Viktor Scuka. Corona from floating electrodes. *Journal of Electrostatics*, 37(12):67 – 78, 1996.
- T. Suzuki, K. Miyake, and T. Hara. Breakdown process in rod-to-plane gaps with dc voltages. *IEEE Transactions on Industry Applications*, IA-21(1):26– 34, 1985.
- T Takuma and T Kawamoto. Numerical calculation of electric fields with a floating conductor. *IEEE Transactions on Di*, 4(2):177 – 181, April 1997.
- Task Force 07.02 of CIGRE Study Committee 33: Britten, Fonseca, Garbagnati, Hutzler, Zheng-Jianchao. Strength of external insulation during live line maintenance and repair work with special reference to transient overvoltages. *Electra*, 129:108–131, March 1990.
- Ryan Andrew Viljoen. Flashover performance of a rod-rod gap containing a floating rod under switching impulse conditions. Master's thesis, School of Electrical & Information Engineering, University of the Witwatersrand, 2008.
- H.H. Zahraee. Proposed theory for streamer-to-leader-transition in non-uniform field air gaps subjected to positive switching-impulses. In *Industry Applications Society Annual Meeting, 1993., Conference Record of the 1993 IEEE*, pages 1653 –1657 vol.3, oct 1993.

Appendix A

Complete set of results from laboratory work

Table A.1: Results, environmental conditions and calculated correction factor for laboratory work with a positive DC voltage and a 500 mm air gap

FC position	**Shot**	**Breakdown voltage (kV)**	**Atmospheric conditions**
No object	1	203.9	Temperature: 23°
	2	204.0	Pressure: 827 mBar
	3	203.0	Relative humidity: 57%
	4	204.3	**Correction factor: 0.8558**
	5	203.7	
25%	1	207.4	Temperature: 25°
	2	208.0	Pressure: 834 mBar
	3	203.1	Relative humidity: 44%
	4	207.3	**Correction factor: 0.8260**
	5	208.0	
50%	1	217.7	
	2	218.3	
	3	217.0	
	4	217.1	
	5	218.3	
75%	1	227.9	
	2	233.3	
	3	229.0	
	4	227.3	
	5	225.7	

Table A.2: Results, environmental conditions and calculated correction factor for laboratory work with a negative DC voltage and a 175 mm air gap

FC position	**Shot**	**Breakdown voltage (kV)**	**Atmospheric conditions**
No object	1	318.1	Temperature: 26°
	2	318.4	Pressure: 833 mBar
	3	318.3	Relative humidity: 43%
	4	318.2	**Correction factor: 0.8407**
	5	317.7	
25%	1	324.0	Temperature: 26°
	2	326.4	Pressure: 833 mBar
	3	330.5	Relative humidity: 43%
	4	325.5	**Correction factor: 0.8322**
	5	325.1	
50%	1	335.7	Temperature: 26°
	2	337.8	Pressure: 833 mBar
	3	338.6	Relative humidity: 43%
	4	333.0	**Correction factor: 0.8273**
	5	335.1	
75%	1	359.3	
	2	359.6	
	3	354.2	
	4	359.2	
	5	355.2	

A complete set of the results obtained during laboratory work is presented along with the environmental conditions that the work was conducted in. The results include both those which have, and have not been corrected for environmental conditions. This acts as a supplement for **Chapter 5**.

Table A.3: Results, environmental conditions and calculated correction factor for laboratory work with a negative DC voltage and a 175 mm air gap

FC position	**Shot**	**Breakdown voltage (kV)**	**Atmospheric conditions**
No object	1	198.2	Temperature: 23°
	2	192.2	Pressure: 836 mBar
	3	187.0	Relative humidity: 53%
	4	197.1	**Correction factor: 0.8169**
	5	200.9	
25%	1	186.3	Temperature: 23°
	2	184.5	Pressure: 836 mBar
	3	177.4	Relative humidity: 47%
	4	184.9	**Correction factor: 0.8169**
	5	180.1	
	6	180.6	
	7	185.3	
50%	1	167.7	
	2	167.0	
	3	165.8	
	4	167.3	
	5	172.6	
	6	174.1	
	7	166.6	
75%	1	115.0	
	2	110.3	
	3	108.6	
	4	114.6	
	5	113.1	
	6	112.9	
	7	114.2	

Table A.4: Results, environmental conditions and calculated correction factor for laboratory work with a negative DC voltage and a 175 mm air gap

FC position	Shot	Breakdown voltage (kV)	Atmospheric conditions
No object	1	268.4	Temperature: 26°
	2	268.8	Pressure: 832 mBar
	3	265.4	Relative humidity: 42%
	4	270.8	**Correction factor: 0.8048**
	5	272.3	
12.5%	1	241.4	Temperature: 25°
	2	240.6	Pressure: 834 mBar
	3	244.3	Relative humidity: 45%
	4	236.9	**Correction factor: 0.8095**
	5	242	
	6	239.8	
	7	245.4	
	8	244.7	
	9	243.6	
	10	241.3	
25%	1	258.6	
	2	262.7	
	3	260.7	
	4	262.4	
	5	260.8	
	6	263.3	
	7	258.8	
	8	264.4	
	9	265.9	
	10	263.0	
37.5%	1	219.4	
	2	256.3	
	3	259.3	
	4	262.2	
	5	214.1	
	6	272.0	
	7	268.7	
	8	257.4	
	9	276.7	
	10	261.4	

FC position	Shot	Breakdown voltage (kV)	Atmospheric conditions
50%	1	265.9	Temperature: 23°
	2	263.0	Pressure: 836 mBar
	3	259.1	Relative humidity: 47%
	4	266.3	**Correction factor: 0.8169**
	5	267.1	
	6	263.5	
	7	263.9	
	8	261.8	
	9	257.3	
	10	262.7	
62.5%	1	190.2	
	2	253.1	
	3	191.5	
	4	192.9	
	5	199.6	
	6	247.7	
	7	238.9	
	8	189.9	
	9	243.0	
	10	186.8	
75%	1	163.4	
	2	161.2	
	3	164.9	
	4	161.5	
	5	159.6	
	6	160.2	
	7	161.6	
	8	158.9	
	9	157.2	
	10	158.5	
87.5%	1	120.3	
	2	122.4	
	3	124.1	
	4	157.1	
	5	161.1	
	6	123.1	
	7	122.1	
	8	120.0	
	9	162.4	
	10	121.2	

Appendix B

Simulation script

The implementation of the simulation work within *MATLAB* and *femm 4.2* is presented. This acts as a supplement for **Chapter 4.**

```
%Model of live-line scenario Code by Craig L. Hart (Wits University, MSc)


%%%%
%Find the critical breakdown voltage of the gap as a function of the
%position of the floating conductor
%%%%


function [Vbd d1] = findCriticalGap(d, step, polarity)
%gap length 1050 or 500(mm)
%steps (12.5mm or 25mm) for movement of the floating conductor (mm)
%polarity: 1 = positive, 0 = negative

d0 = 250; %length of the floating conductor (mm)

Vbd((d-d0)/step + 1) = 0; %declares holding matrix for BD voltage
bd_case((d-d0)/step + 1) = 0; %matrix for showing the case of BD

Vbd1((d-d0)/step + 1) = 0; %matrix of the critical voltage of gap 1
Vbd2((d-d0)/step + 1) = 0; %matrix of the critical voltage of gap 2
k0((d-d0)/step + 1) = 0;

for d1 = 0:step:d-d0 %Increments the primary gap size/FC position

    d2 = d-d0-d1;

    k = getFloatingPotential(d,d1,1); %Coeffecient for geometrically
                                      %induced voltage


    Vb1 = getPrimaryVBD(d1,polarity); %BD voltage of the primary gap
    Vb2 = getSecondaryVBD(d2,polarity); %BD voltage of the secondary gap

    V_hv = Vb1/(1-k); %V_hv is set to just breakdown the primary gap
    V_fc = k*V_hv; %V_fc is then calculated

    if Vb2 < V_fc %BD of Gap 2 occurs prior to Gap 1

        %Assign Vb2 to V_fc, and calculate V_hv in order to find the lowest
        %applied BD voltage

        V_fc = Vb2; %As Gap 2 breaks down
        V_hv = V_fc/k;

        if V_hv <= Vb1
            Vbd(d1/step + 1) = V_hv;
            bd_case(d1/step + 1) = 0; %breakdown of Gap2 leads to immediate
               %BD of Gap1. i.e. Gap 2's strength is the determining factor
        else
            V_hv = Vb1;
            Vbd(d1/step + 1) = V_hv;
            bd_case(d1/step + 1) = 1; %partial BD of Gap 2 occurs,
            %grounding FC. Thus, Vb1 becomes the determing voltage
        end
```

```
    elseif Vb2 >= V_fc && Vb2 <= V_hv
        Vbd(d1/step + 1) = V_hv;
        bd_case(d1/step + 1) = 2; %Simultaneous BD of both gaps, i.e. Gap 1
                                  %leads to immediate BD of Gap 2
    else
        Vbd(d1/step + 1) = Vb2;
        bd_case(d1/step + 1) = 3; %Partial BD of the primary gap occurs
            %until V_hv > Vb2. Thus Vb2 becomes the determining voltage
    end


    if d1 == 0
       Vbd(d1/step + 1) = Vb2;
    elseif d2 == 0
       Vbd(d1/step + 1) = Vb1;
    end

    Vbd1(d1/step + 1) = Vb1;
    Vbd2(d1/step + 1) = Vb2;
end
```

```
%Model of live-line scenario
%Code by Craig L. Hart (Wits University, MSc)


%%%%
%Get the floating potential of the FC
%%%%


function V_FC = getFloatingPotential(d,d1,polarity)

openfemm
newdocument(1)

%d = 750; %total gap length
%d1 = 150; %primary gap length (to be varied)
rSphere = 75; %floating sphere radius
hRod = 500; %HV rod height
rRod = 9; %radius of the rod
hTip = 9/tan(15*pi/180); %height of the conical tip of the rod
hPro = 100; %height of the protrusion
rPro = 2.5; %radius of the protrusion
xPlane = 2000; %length of the plane
hPlane = 2; %height of the plane

% Define the problem type.  Magnetostatic; Units of mm; Axisymmetric;
% Precision of 10^(-8) for the linear solver; a placeholder of 0 for
% the depth dimension, and an angle constraint of 30 degrees


ei_probdef('millimeters','axi', 10^(-8), 0, 30);

% draw geometry of interest
    %Plane
ei_drawline(0,0, xPlane/2,0);
ei_drawline(xPlane/2,0, xPlane/2,-hPlane);
ei_drawline(xPlane/2,-hPlane, 0,-hPlane);

    %Rod and tip
ei_drawline(0,d, rRod,d+hTip);
ei_drawline(rRod,d+hTip, rRod,d+hTip+hRod);
ei_drawline(rRod,d+hTip+hRod, 0,d+hTip+hRod);

        %Sphere and protrusion
if polarity == 1
%positive
    ei_drawline(0, d-d1-2*rSphere-hPro, rPro, d-d1-2*rSphere-hPro);
    ei_drawline(rPro, d-d1-2*rSphere-hPro,
                rPro, d-d1-rSphere*(1 + sin(acos(9/75))));
    ei_drawarc(rPro, d-d1-rSphere*(1 + sin(acos(9/75))),
                rSphere, d-d1-rSphere, acosd(9/75),1);
    ei_drawarc(rSphere,d-d1-rSphere, 0,d-d1, 90,1);
else
%negative
```

```
    ei_drawarc(0,d-d1-hPro-2*rSphere, rSphere, d-d1-hPro-rSphere, 90,1);
    ei_drawarc(rSphere,d-d1-hPro-rSphere,
                rPro,d-d1-hPro-rSphere*(1-sin(acos(9/75))), acosd(9/75),1);
    ei_drawline(rPro,d-d1-hPro-rSphere*(1-sin(acos(9/75))), rPro, d-d1);
    ei_drawline(rPro,d-d1, 0,d-d1);
end
    %Draw large region boundary and interconnecting lines
ei_drawarc(0,-750, 0,2000, 180,2);

ei_drawline(0,-750, 0,-hPlane);
ei_drawline(0,0, 0,d-d1-2*rSphere-hPro);
ei_drawline(0,d-d1, 0,d);
ei_drawline(0,d+hTip+hRod, 0,2000);

ei_drawline(0,-750, 0,2000);



%-------------------------------------------------------%

%Add block labels for conductors and mark them with "No Mesh"
%Note: all objects are labelled as close to the geometric centre as poss.

if polarity == 1
    ei_addblocklabel(rSphere/2,d-d1-rSphere); %FC
    ei_selectlabel(rSphere/2,d-d1-rSphere);
else
    ei_addblocklabel(rSphere/2,d-d1-hPro-rSphere); %FC
    ei_selectlabel(rSphere/2,d-d1-hPro-rSphere);
end
ei_setblockprop('<No Mesh>',0,100,0); %100mm mesh element size
ei_clearselected;


ei_addblocklabel(rRod/2,d+hRod/2); %Rod
ei_selectlabel(rRod/2,d+hRod/2);
ei_setblockprop('<No Mesh>',0,100,0); %100mm mesh element size
ei_clearselected;

ei_addblocklabel(xPlane/4,-hPlane/2); %Plane
ei_selectlabel(xPlane/4,-hPlane/2);
ei_setblockprop('<No Mesh>',0,100,0); %100mm mesh element size
ei_clearselected;

% Add and assign the block labels for the air region
ei_addmaterial('air',1,1,0);
ei_addblocklabel(500,d/2); %some point in air (halfway of gap)
ei_selectlabel(500,d/2);
ei_setblockprop('air',0,100,0); %100mm mesh element size
ei_clearselected;



% Add a "Conductor Property" for each of geometries
```

```
ei_addconductorprop('FC',1,0,1);
ei_addconductorprop('Plane',0,0,1);
ei_addconductorprop('Rod',0,0,1);


% Assign the Rod and 0V properties to the rod
    %Select all line segments of the rod at midway
ei_selectsegment(0, d+(hTip+hRod)/2);
ei_selectsegment(rRod/2, d + hTip + hRod);
ei_selectsegment(rRod,d + hTip + hRod/2);
ei_selectsegment(rRod/2, d + hTip/2);

    %Assign
ei_setsegmentprop(0,0.1,0,0,0,'Rod');
ei_clearselected

%Assign the 0V and Plane properties to plane conductor
    %selection of the plane line segments
ei_selectsegment(xPlane/4,0);
ei_selectsegment(xPlane/4,-hPlane);
ei_selectsegment(0,-hPlane/2);
ei_selectsegment(xPlane/2,-hPlane/2);

    %Assign
ei_setsegmentprop(0,1,0,0,0,'Plane');
ei_clearselected

%Assign floating conductor properties
    %Arc segment
ei_selectarcsegment(0,d-d1);

    %Assign
ei_setarcsegmentprop(0.25,0,0,0,'FC');
ei_clearselected;

    %Protrusion section
ei_selectsegment(0,d-d1-rSphere-hPro/2);
ei_selectsegment(rPro/2, d-d1-2*rSphere-hPro);
ei_selectsegment(rPro, d-d1-2*rSphere-hPro/2);

    %Assign
ei_setsegmentprop(0,0.1,0,0,0,'FC');
ei_clearselected;

%Put everything in perspective
ei_zoomnatural;

% Save the geometry to disk so we can analyze it
ei_saveas('FC_axisymm.fee');

% Analyze the problem
ei_analyze
%
% Load the solution
```

```
ei_loadsolution


CP = eo_getconductorproperties('Rod');
Q1= CP(2);
CP = eo_getconductorproperties('Plane');
Q2= CP(2);
Q3 = eo_getconductorproperties('FC');
Q3= CP(2);

C1 = Q1;
C2 = Q2;
C3 = Q3;

V_FC = abs(C1/C3);

end
```

```
%Model of live-line scenario
%Code by Craig L. Hart (Wits University, MSc)


%%%%
%Calculate the breakdown voltage of a rod-rod gap for the primary gap
%%%%


function Vbd = getPrimaryVBD(d1,polarity)

    h=11; %Humidity under standard conditions (g/m^3)

    if polarity == 1
        A = 20; %kV
        B = 5.1/10; %kV/mm
    else
        A = 15; %kV
        B = 5.45/10; %kV/mm
    end

    Vbd = (A+B*d1)*nthroot(5.1e-2*(h+8.65),4); %Formula for a rod-rod gap

end
```

```
%Model of live-line scenario
%Code by Craig L. Hart (Wits University, MSc)


%%%%
%Calculate the breakdown voltage of a rod-plane gap for the secondary gap
%%%%


function Vb2 = getSecondaryVBD(d2,polarity)

    if polarity == 1
        Es = 500/1000; %kV/mm
    else
        Es = 1200/1000; %kV/mm
    end

    Vb2 = Es*d2;

end
```

Appendix C

Conference submission to ISH 2011

A paper by the author that contributes towards **Chapter 2** is included. This paper was presented at the 17^{th} International Symposium on High Voltage Engineering (ISH) in 2011 and can also be found in the conference proceedings.

INITIAL RESEARCH INTO QUANTIFYING THE EFFECT OF A SUSTAINED DC FIELD ON BREAKDOWN PHENOMENA USING HIGH-SPEED PHOTOGRAPHY

C. L. Hart[1*], K. J. Nixon[1] and I. R. Jandrell[1]
[1]School of Electrical & Information Engineering, University of the Witwatersrand, Johannesburg, South Africa
*Email: <craig.hart@students.wits.ac.za>

Abstract: The importance of High Voltage Direct Current (HVDC) transmission lies in the fact that it is the only economically feasible option for power transmission over vast distances. As a result, the nature of HVDC transmission lines, and in particular the effect of the sustained field surrounding these lines, must be understood. In order to gain a better understanding of the effect of the sustained field surrounding these lines, the breakdown of air in a rod-plane gap was investigated under electrical stress of DC voltages of both polarities up to approximately 250 kV. Tests were done at an altitude of 1742 m in Johannesburg, South Africa. Results show that for negative DC voltages, breakdown of the gap required significantly higher voltages than that for positive polarity. This is suggested to be a result of the effect of the sustained field on space charge within the gap. High-speed photography (up to 775 000 frames per second) of breakdown with both polarities allowed analysis of visual evidence of the breakdown. The observed visible streamers differed considerably for both polarities, with the streamer propagating much further into the gap prior to breakdown under positive polarity and the formation of a second streamer branch.

1 INTRODUCTION

The number of proposed High Voltage Direct Current (HVDC) projects worldwide, as well as in Africa, is due to it being economical for transmitting power over long distances when compared to High Voltage Alternating Current (HVAC) power distribution [1]. Hydroelectric projects in particular lead to vast distances between the energy source (a dam) and consumer. For example, to import power from the Inga hydroelectric project would require close to 4000 km of transmission line, which is only realistically feasible by use of HVDC transmission lines [1]. With South Africa's national power utility, Eskom, investigating the importation of power from the Inga project, as well as importing additional power on the existing Cahora Basa line, an understanding of HVDC power transmission is vital.

While the field conditions surrounding HVAC lines have been extensively researched, this is not the case for HVDC lines. With HVDC lines, there are three types of configurations, namely monopolar, bipolar and homopolar. With these three types of configurations, the conductors can be at either positive or negative polarity, or with a conductor at each polarity as in the case of bipolar lines [2]. This results in HVDC lines with a sustained field at both polarities, leading to the constant presence of space charge which distorts the field, changing the critical values of breakdown for different geometries [3]. The polarity of the DC voltage also has an effect on the field distortion due to the behaviour of the space charge in a reversed field [3], leading to an increased number of factors which must be investigated in order to better understand HVDC transmission

In this paper, research is presented that aims at understanding the effect of a sustained field from HVDC on breakdown phenomena at both polarities. In particular the effect of this sustained field at high altitudes is investigated, with the research conducted at an altitude of 1742 m in Johannesburg, South Africa. The use of high-speed photography, with a maximum time resolution of approximately 1.29 μs is also employed in order to provide visual evidence of the breakdown under DC conditions.

2 METHODOLOGY

In order to aid the design of efficient and maintainable HVDC lines, it is important to understand the nature of air breakdown due to strong electric fields resulting from HVDC. Therefore, the research presented in this paper focuses on the analysis of fundamental breakdown principles when applied to a HVDC scenario. In particular, the research investigates the effect of a sustained field and the constant presence of space charge on air breakdown within a rod-plane gap. With the laboratory work having been done in Johannesburg, it also serves as an investigation into these breakdown phenomena at high altitude, with the laboratory at an altitude of approximately 1742 m.

The laboratory work involved looking at the breakdown voltage of a rod-plane gap as a function of the gap size, for both positive and negative DC voltages. In addition to these physical measurements, a high-speed camera was used to record visual evidence of the occurring breakdown phenomena.

3 EXPERIMENTAL SET-UP

A diagram of the experimental set-up is represented in Figure 1. An HVDC generator that is rated at 400 kV and 15 mA (however limited to 250 kV at the time of testing) was used to energise a rod-plane gap. An aluminium rod with a diameter of 16 mm and a rounded tip was used. The plane is approximated by a 1.2 x 2.1 m steel mesh. A labelled photograph of the test set-up in the laboratory is shown in Figure 2.

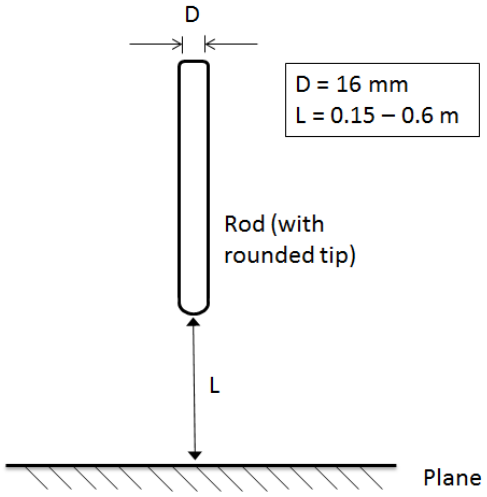


Figure 1: Diagram of the experimental set-up used for testing



Figure 2: Photograph of the test set-up at the HV Laboratory at the University of the Witwatersrand

4 TESTING CONDITIONS AND RESULTS

Tests have been conducted at the High Voltage Laboratory at the University of the Witwatersrand, Johannesburg. Atmospheric conditions during testing were recorded, and are presented in Table 1, along with the calculated relative air density. A correction factor is used to obtain a value of breakdown voltage at standard conditions, as defined by IEC standards [4], and is shown in Equation 1,

$$V = KV_0 \quad (1)$$

where V is the measured breakdown voltage, V_0 is the breakdown voltage in standard conditions and K is the correction factor, which is further defined in Equation 2,

$$K = k_1 k_2 \quad (2)$$

where k_1 is the air density correction factor and k_2 is the humidity correction factor [4]. For the purposes of this paper, k_1 is the equivalent of the relative air density while k_2 is ignored due to a lack of consensus on the effect of humidity on DC breakdown voltages and its application to the different polarities of DC voltage [5].

Table 1: Environmental conditions and correction factors measured during testing

Parameter	Value
Temperature (°C)	15
Pressure (mBar)	827
Relative humidity (%)	28
Relative air density	0.83

One of the main issues encountered during testing was establishing an accurate measurement of the breakdown voltage. The breakdown voltage was measured using the voltmeter on the control panel of the HVDC generator. The shortfall of this measurement is that there is no way to interface it with a 'trigger and hold' measurement. As a result, a suitable approach had to be taken so that there were very small increments on the output around the breakdown voltage of the gap, in order to ensure a more accurate measurement. The approach used for taking each measurement is outlined in Figure 3. The results from testing are presented in Figure 4, with the corrected values of breakdown voltage for both polarities plotted as a function of the gap size, alongside published data from Suzuki et al [6].

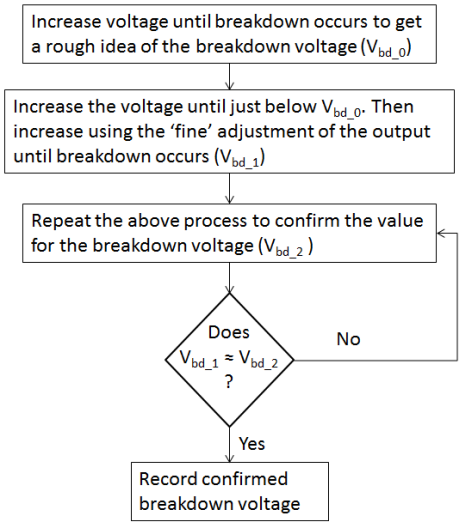


Figure 3: Process flow diagram for recording the breakdown voltage for each gap size

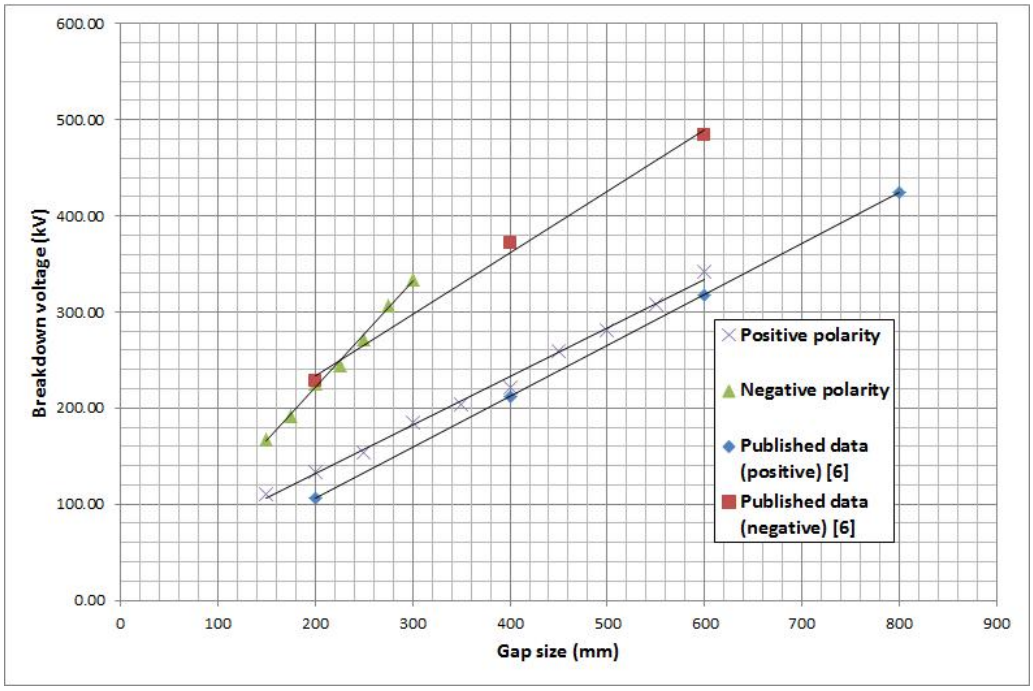


Figure 4: Breakdown voltage as a function of gap size for DC voltages of both polarities in a rod-plane gap, alongside data from [6]

5 HIGH SPEED PHOTOGRAPHY

High-speed photography was performed with a Photron SA5 high-speed camera [7] in order to obtain visual evidence of the breakdown of the gap under DC voltages at both polarities. To record breakdown under a positive DC voltage, a gap size of 350 mm was used with a frame rate of 525 000 frames per second. Five sequential, processed and colour-inverted photographs are presented in Figure 5, with breakdown of the gap shown in Figure 5(e). Breakdown under a negative voltage was recorded for a 250 mm gap size, with an increased frame rate of 775 000 frames per second. The processed and inverted photographs are presented in Figure 6, with three sequential frames of significant images obtained, with breakdown of the gap shown in Figure 6(c).

A time and distance scale is included in both Figures 4 and 5. The distance is along the rod-plane axis into the gap and is calculated from using the knowledge of the rod's diameter as a size reference. A graphical plot of visible streamer progression into the gap as a function of time for both negative and positive polarities is presented in Figure 6. Within Figure 6, the relevant frames in both Figures 4 and 5 are labelled on the graph. Note that the point at which Figure 5(d) occurs is not included in this graph due to progression of visible streamers being beyond the area of the frame. This may also be the case for the point at which Figure 5(c) occurs; however this point has still been included in the plot.

6 ANALYSIS OF RESULTS

Results are shown in Figure 3 alongside published data by Suzuki et al [6], which are from tests performed at sea level. From Figure 3, it is clear that breakdown of the gap occurs at much higher voltages for negative voltages as opposed to positive voltages with the same gap size. This is a trend that is consistent with the data from [5]. This can be explained by the influence of space charge within the gap.

With a non-uniform field, such as that in a rod-plane gap, breakdown occurs at much lower voltages, due to a localised high field region [8]. In the case of a rod-plane gap, this is close to the rod. With a positive DC voltage, the electrons formed during ionisation will move towards the rod, while the less-mobile positive ions remain within the gap. These ions distort the field, increasing the field at the tip of the space charge, and as the ions slowly move towards the earthed plane, the region in which ionisation can take place is extended further into the gap [3]. When a negative DC voltage is applied to the gap, the electrons from initial ionisation move towards the earthed plane, while positive ions remain close the negative rod. This leads to a highly enhanced field close to the rod, and a reduced field in the gap, resulting in a decreased region that ionisation can take place in. A result of this is that a higher voltage is required for breakdown of the gap [3].

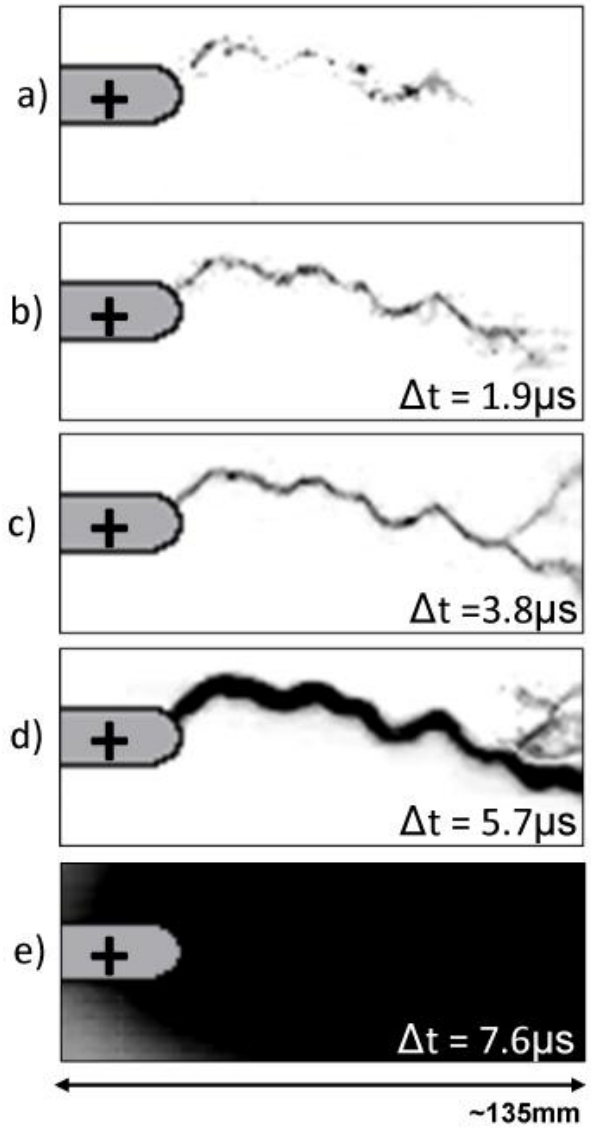


Figure 5: Processed and colour-inverted photographs of the breakdown of a 350 mm rod-plane gap under a positive DC voltage at 525 000 frames per second

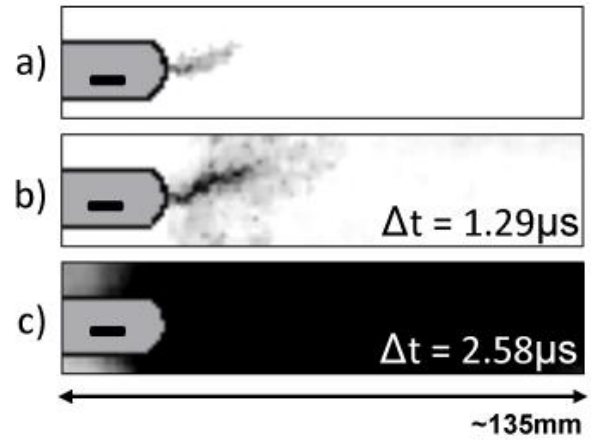


Figure 6: Processed and colour-inverted photographs of the breakdown of a 250 mm rod-plane gap under a negative DC voltage at 775 000 frames per second

From Figure 5, it can be seen that the visible streamer progresses much further into the gap prior to breakdown. Also, the formation of a second streamer branch approximately 80 mm into the gap, shown initially in Figure 5(b), and its development in Figures 5(c) and 5(d), suggests that there is additional ionisation further into the gap.

In Figure 6, it is clear that the visible streamer does not progress far from the region around the rod before breakdown of the gap occurs. Using Figure 7 to quantify the visible streamer progression in relation to time for both polarities, it becomes evident that the visible negative streamer does not propagate much further than approximately 22 mm from the rod before breakdown. This is in comparison to the progression of the positive streamer to approximately 103 mm, with a further 3.8 μs before breakdown. The inclusion of the extra frame of Figure 5(d) prior to breakdown suggests that the streamer propagates even further into the gap.

The reason for the difference in distance that each polarity's visible streamer propagates into the gap is not clear; however it is possible that it is due to the aforementioned difference in the size of the regions of ionisation due to the effect of space charge in the sustained field. If there is less ionised air in the gap due to the smaller ionisation region of a negative rod-plane gap, this could lead to less visible streamers in the gap prior to breakdown. With this observation, it should be reminded that as two different gap lengths were recorded, further experiments will have to be conducted with similar conditions in order to confirm that the differences are related to the polarity of the applied voltage to the gap.

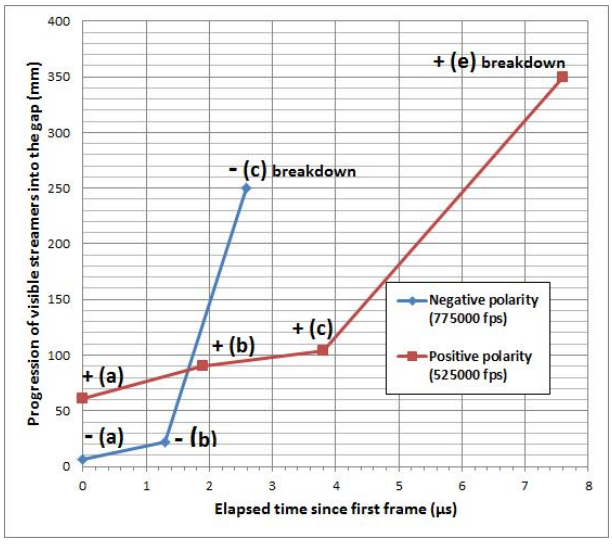


Figure 7: Visible streamer progression into the gap as a function of time for breakdown under both polarities

7 CONCLUSION

The breakdown of air in a rod-plane gap under DC voltages was investigated. Tests were conducted at 1742 m at the University of the Witwatersrand. The gap sizes ranged between 150 and 600 mm for positive DC voltages, and 150 and 300 mm for negative DC voltages. Results showed that a significantly higher voltage was required to breakdown the same gap size for a negative DC voltage relative to a positive DC voltage. This result is consistent with other published data from tests performed at sea level, which is also presented. The significant difference in breakdown voltage at either polarity was explained in terms of space charge, and the effect the sustained DC field has on the space charge in the gap. Visual evidence of the breakdown of the rod-plane under both polarities was obtained using high-speed photography, with a time resolution of 1.9 μs and 1.29 μs obtained for positive and negative polarity respectively. From these photographs, a difference in the distance of propagation of a visible streamer into the gap prior to breakdown was observed for both DC voltage polarities. The visible positive streamer progressed much further into the gap than the visible negative streamer. A second streamer was also shown to form within the gap under a positive voltage.

8 ACKNOWLEDGMENTS

The authors would like to thank Eskom for the support of the High Voltage Engineering Research Group through the TESP programme. They would also like to thank CBI-electric for support, the department of Trade and Industry (DTI) for THRIP funding as well as to the National Research Foundation (NRF) for direct funding.

9 REFERENCES

[1] A. Britten, L. Pillay, P. Naidoo, F. Bologna, D. Muftic, N. Ijumba: “Eskom’s proposed strategic research into HVDC transmission”, Energize, July 2005

[2] N. Ijumba, G. Sibilant. The planning, design and construction of overhead powerlines, Crown Publications cc, February 2005, ch. 4, pp. 68–92

[3] E. Kuffel, W. Zaengl, J. Kuffel. High Voltage Engineering: Fundamentals, 2nd ed. Newnes, 2000

[4] “High voltage test techniques, part 1. General definitions and requirements”, IEC 60-1, 1990

[5] P.A. Calva, V. del Moral, M.G. Márquez, G.P. Cabrera: “New Proposal of Correction Factors for DC Voltages”, Annual Report Conference on Insulation and Dielectric Phenomena, pp. 455- 458, 2003

[6] T. Suzuki, K. Miyake, T. Hara: “Breakdown Process in Rod-to-Plane Gaps with DC Voltages”, IEEE Transactions on Industry Applications, Vol. IA-21, No. 1, pp. 26- 34, 1985

[7] Photron: High Speed Video Camera for Slow Motion Analysis, url: http://www.photron.com, last accessed: June 07, 2011

[8] N.L. Allen, M. Boutlendj: "Study of the electric fields required for streamer propagation in humid air", Science, Measurement and Technology, IEE Proceedings A, Vol. 138, No.1, 1991

Appendix D

Conference submission to PowerAfrica 2012

A paper by the author that is based on the presented work is included. This paper was presented at IEE PES Power Africa 2012.

IEEE PES POWERAFRICA 2012 CONFERENCE AND EXPOSITION
JOHANNESBURG, SOUTH AFRICA, JULY 9–13, 2012

The effect of a floating conductor on the breakdown strength of a DC gap at both polarities

C.L. Hart, K.J. Nixon and I.R. Jandrell
School of Electrical & Information Engineering, University of the Witwatersrand
Private Bag 3, 2050, Johannesburg, South Africa.
Email: craig.hart@students.wits.ac.za

***Abstract*—This paper presents a preliminary investigation into the effect of a floating conductor on the breakdown strength of a rod-plane gap energised by both positive and negative polarities. This experiment models the scenario of live-line maintenance, therefore providing results for a research into HVDC live-line maintenance, with special reference to the existing HVDC lines and proposed future projects in Southern Africa. The experimental work makes use of a floating conductor comprised of a copper sphere and a rod protrusion on the anodic side of the sphere, based on conclusions from previous research. The experimental work is split into two main parts with positive and negative DC voltages. The experimental work determines the U_{50} breakdown voltage of a rod-plane gap as the floating conductor is moved within the gap. A comparison of the change in the breakdown strength of the gap is made against the base case of a rod-plane gap with no object and a gap size which is equal to the split gap size. The U_{50} breakdown voltage is then presented as a function of the primary gap (energised rod to floating conductor) size. From the positive polarity results, it is evident that the presence of a floating conductor raises the DC breakdown strength of the gap, with the breakdown strength increasing almost linearly as the primary gap is increased. A completely different effect is observed with the presence of a floating conductor in a negative DC gap. The presence of a floating conductor immediately lowers the breakdown strength of the gap, and there is a sharp decline in the breakdown strength as the object approaches the ground plane. This result suggests that the implementation of live-line maintenance on HVDC lines would have to consider two completely separate guidelines to deal with positive and negative HVDC lines respectively.**

***Index Terms*—Power, Transmission, HVDC, Live-line Maintenance, Floating Conductor, Space Charge, Rod-Plane, Polarity.**

I. INTRODUCTION

High Voltage Direct Current (HVDC) transmission is becoming increasingly more significant in worldwide transmission networks. Within South Africa alone, there is the Cahora Bassa line which runs 1400 km from the Cahora Bassa dam in Mozambique to the Apollo converter station in Johannesburg and is responsible for importing 1800 MW of hydroelectric power into South Africa (SA) from Mozambique [1]. Additionally in Southern Africa, there is the Caprivi Link in Namibia, which imports 350 MW of power from Zambia [2]. These are just the active HVDC lines in Southern Africa, while there are currently eight proposed HVDC transmission lines in Eskom's latest Transmission Development Plan (TDP) for 2012, there are five HVDC line projects that are currently deferred but still planned, including an 800 kV line from Lephale in Limpopo to Durban [3]. The advantage HVDC offers as a transmission tool, is a more economical power transmission over long distances than High Voltage Alternating Current (HVAC) [4].

Worldwide, many power utilities perform live-line maintenance on their power transmission and distribution networks in order to minimise line downtime and maximise power throughput on the network. As it stands, the IEEE standard for live-line maintenance does not differentiate clearly between the requirements for live-line maintenance on AC or DC lines [5]. The challenging aspect about live-line working on a DC lines is that the effect of a sustained DC field at both polarities, is not well understood and in the case of live-line working, safety of the workers is of paramount importance. The polarity of the DC voltage also has an effect on the field distortion due to the behaviour of the space charge in a reversed field [6], leading to an increased number of factors which must be investigated in order to better understand HVDC transmission.

This paper presents a investigation into the effect of a sustained DC field on the breakdown strength of a non-uniform air gap when a floating conductor is inserted into the gap, and its position is varied. Furthermore, the experimental work presented was performed in Johannesburg at an altitude of 1732 m, meaning that the research specifically investigates the scenario of live-line maintenance in conditions of reduced air density.

II. MODEL OF LIVE-LINE MAINTENANCE

Previous research has been done into live-line maintenance, whereby focus has been on the breakdown strength of air gaps in the presence of switching impulse overvoltages. Rizk [7], Hutzler [8] and Baldo and Pesavento [9] all modelled the scenario of live-line maintenance using a Floating Conductor (FC) in a non-uniform gap. The aforementioned research was then consolidated in a working report by CIGRE [10]. The case of a FC inserted into a non-uniform gap aims to model several cases of live-line maintenance such as a worker on a metal platform, a worker in a conductive suit and an approaching helicopter.

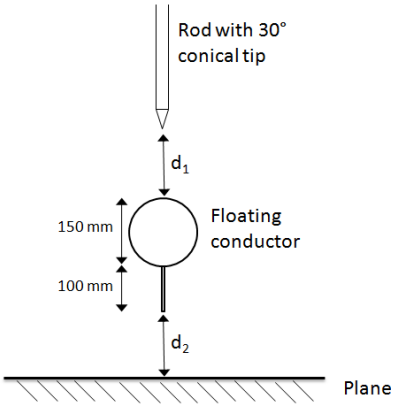
The aforementioned research, however, only considered switching overvoltages as its focus was toward live-line maintenance on High Voltage Alternating Current (HVAC) lines. With the case of HVDC, there are two important parameters which have to be considered. These are namely a sustained field from the voltage on the line itself and the polarity of that voltage. These two added complexities will be provisionally explored in the following sections.

III. EXPERIMENTAL PROCEDURE

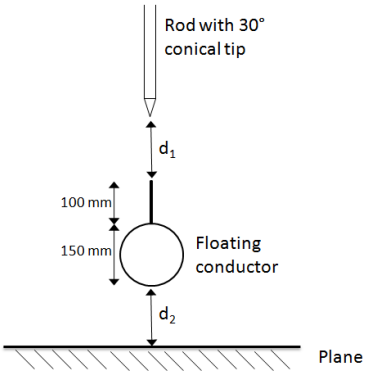
A. Experimental set-up

In order to model the scenario of live-line maintenance, a FC is inserted into a non-uniform field. For all experimental work, a 150 mm diameter copper sphere with a 100 mm protrusion was employed. The geometrical specifications of the sphere are based on past research on floating body potentials and their effect on the breakdown strength of a non-uniform gap [8]. From the conclusions of this work, a sphere with an anodic protrusion is chosen as the FC that would represent the most onerous case of a floating object in an electric field. This choice of FC also attempts to model the imperfect geometry of any floating conductor that may enter a physical air gap surrounding an actual HVDC line, where sharp edges that may act as sources of corona discharge can not be avoided.

The protrusion used in combination with the sphere is a 5 mm diameter square-cut rod. The FC is orientated such that it has an anodic protrusion, as if this is not the case the protrusion does not have any additional effect towards the floating objects decay of the breakdown strength of the gap [8]. This conclusion is from work that did not consider negative polarity, however the result is assumed to be consistent for both polarities. The test set-ups used for positive and negative polarity are shown in Figure 1. In Figure 1, d_1 and d_2 represent the primary and secondary gaps respectively. The combination of the two gaps is referred to as the split gap. All experimental work was done in the High Voltage Laboratory at the University of the Witwatersrand in Johannesburg in reduced air density conditions at an altitude of 1732 m.



(a) Positive, non-inverted set-up



(b) Negative, inverted set-up

Fig. 1. Diagram of the test object with floating conductor for experiments with (a) positive polarity and (b) negative polarity

B. Experimental procedure

The experimental work consists of two main components, namely experiments consisting of positive and negative polarities respectively. The experimental procedure is based on the determination of the U_{50} breakdown voltage of a rod-plane gap with a FC for different positions of the FC within the gap, using the IEC standard for HVDC testing [11]. The U_{50} breakdown voltage is determined by linearly increasing a DC voltage until breakdown occurs and the breakdown voltage being noted. This is repeated five times for each specific set-up, with the average value giving the U_{50} breakdown voltage. The presence of a floating object within the test object, means that the object must be earthed after every application of a shot in order to discharge any residue charge on the object.

The position of the object is identified by either the size of the primary gap (d_1) or the percentage ratio of the primary gap to the split gap ($d_1 + d_2$). For consistency, the position of the FC will be referred to by the latter. The variation of the FC's position in the test gap is in Figure 2, where the position of the conductor is moved in increments of 25%. A base case for comparison of the results is a rod-plane gap with no object and a gap size equal to the split gap size. This is based on the fact that the presence of a FC effectively short circuits the gap over its length in the rod-plane gap. Experimental work included split gap sizes of 50 cm and 17.5 cm for the positive DC and negative DC experiments respectively.

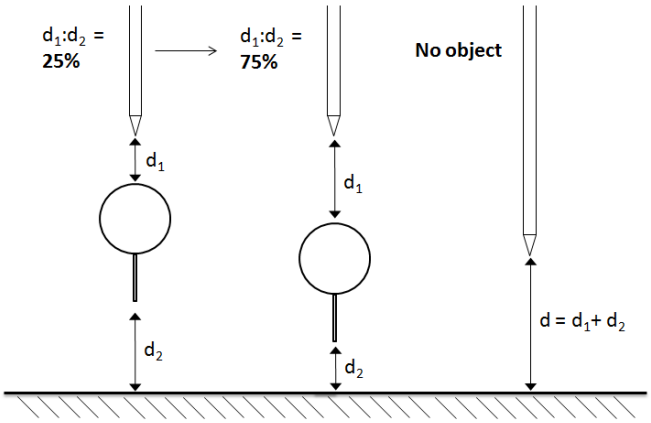


Fig. 2. Test procedure for determination of the breakdown strength of a gap with a floating conductor

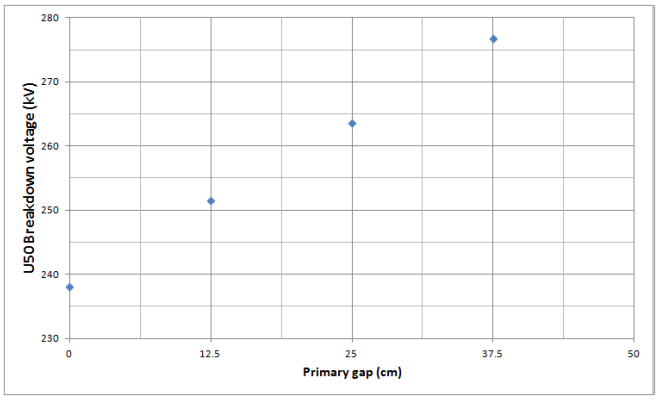


Fig. 3. U_{50} breakdown voltage of a positive DC rod-plane gap a split gap size of 50 cm

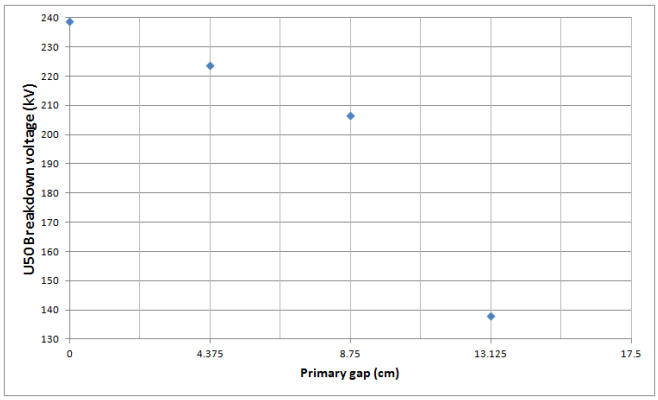


Fig. 4. U_{50} breakdown voltage of a negative DC rod-plane gap with a split gap size of 17.5 cm

IV. RESULTS AND ANALYSIS

A. Overview of results

This experimental work focuses on the the effect of a FC on the breakdown strength of a non-uniform DC gap at both polarities, and the comparison of the two results. The U_{50} breakdown voltage as a function of the primary gap length (and the position of the object in percentage) for a positive DC gap is presented in Figure 3, while that for the negative DC experiment is presented in Figure 4. Note that the data point when the primary gap is zero represents the no object case.

B. Discussion and analysis

The effect of a FC for a rod-plane gap energised by a positive direct voltage is presented in Figure 3. As can be seen in Figure 3, the presence of a FC immediately increases the breakdown strength of the gap when compared to the no-object case. This is the opposite effect of the presence of the FC on a negative DC gap, where it lowers the breakdown strength of the gap.

From Figure 3, it is observed that the breakdown voltage increases as the primary gap increases and the FC is moved towards the ground plane. Figure 4 shows the effect of the position on the breakdown strength of a rod-plane gap energised by a negative direct voltage with an evident decline in the breakdown strength of the gap as the FC approaches the ground plane.

When physically interpreting the results from both tests in this study, it can be seen that the most critical point of the floating object in a positive DC non-uniform field is close to the conductor, while that in a negative DC non-uniform field is close to the ground plane.

This result suggests that the implementation of live-line maintenance on HVDC lines would have to consider two completely separate guidelines to deal with positive and negative HVDC lines respectively. This is in itself is a logical step, as it is well documented in high voltage engineering that the nature of breakdown in non-uniform geometries under different polarities is very different. In

fact, the streamer gradients of the two different polarities under DC stress have been shown to differ by close to a factor of two [12] for a rod-plane geometry. This is due to the interaction of the electrons and ions formed during the breakdown process with the sustained DC field. As the sustained field is in the reverse direction when the polarity is switched, this leads to a different arrangement of the space charge within the gap [6]. The distortion of the field by this space charge therefore is distinct for both polarities, leading to a different breakdown criterion.

This explanation is offered to smaller air gaps where breakdown occurs through the streamer mechanism, while the air gaps on physical transmission line and tower geometries significantly larger, and would expectantly breakdown by the leader mechanism. However, the effect of polarity has also been shown to be present with the leader mechanism in larger air gaps [13]. As the leader mechanism is initiated by elementary streamers, the polarity effect on the formation of these streamers is still valid. Secondly, due to the radial diffusion of electrons and photons during the elementary streamer formation (and avalanche), the channel from which the leader starts and propagates is different at both polarities. In the case of positive streamers, the electrons converge on the streamer head resulting in a narrow channel, while for negative streamers the electrons and photons, produced as the streamer propagates, diverge away from the streamer head causing a much broader channel [13]. This behaviour of the streamer channels results in an effectively blunter curvature of the high voltage source in the case of negative polarity, which will result in a reduced maximum electric field.

The polarity effect on streamer channels is shown in a sequence of high-speed photographs of the breakdown of a rod-plane gap for both positive and negative polarity in Figures 5 and 6 respectively. In Figure 5, there is clearly a defined, narrow channel that propagates into the gap from the energised rod. This is in contrast to the divergent and less-defined channel that propagates under negative DC stress in Figure 6.

It should be noted that the scope of this work does not consider the case of a bipolar line where the two lines, and polarities, are close enough such that there is an interaction between the two electric fields. It also does not consider the case of switching overvoltages on the line and the complete electrical situation that may be present on HVDC lines during live-line maintenance. This scope of work is suggested for further investigation into the scenario of HVDC live-line maintenance.

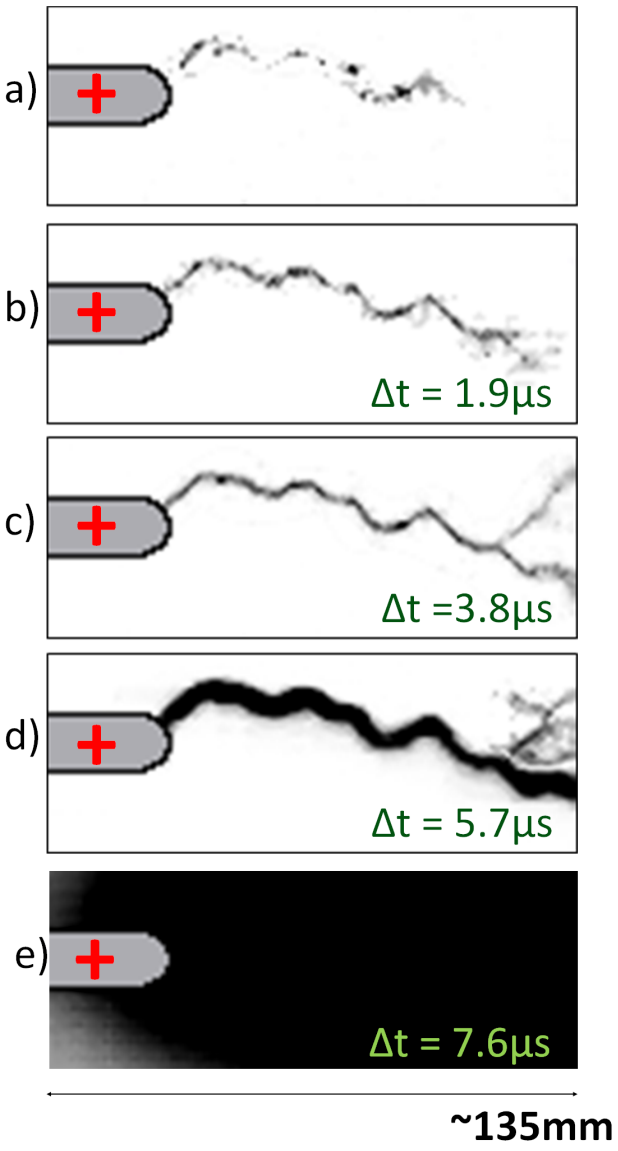


Fig. 5. High-speed photography of the positive DC breakdown of a 350 mm rod-plane gap [12]

V. CONCLUSION

Experimental work was conducted to investigate the effect of a FC on the breakdown strength of a DC gap at both polarities. A FC comprising of a sphere and anodic protrusion was chosen based on previous research on floating bodies. From the positive polarity results, it was evident that the presence of a FC raised the DC breakdown strength of the gap, with the breakdown strength increasing almost linearly as the primary gap is increased.

A completely different effect is observed with the presence of a FC in a negative DC gap. The presence

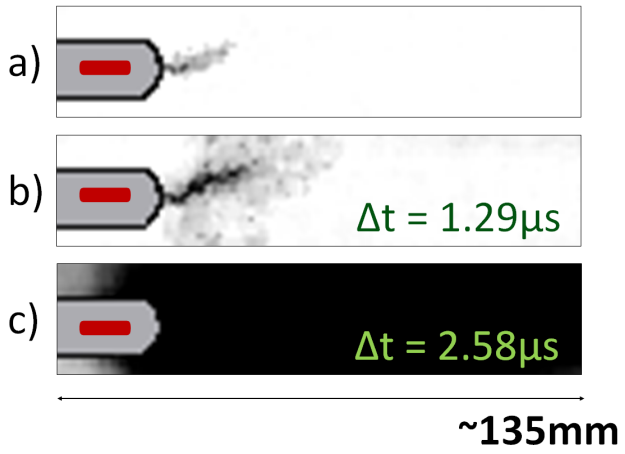


Fig. 6. High-speed photography of the negative DC breakdown of a 250 mm rod-plane gap [12]

of a FC immediately lowers the breakdown strength of the gap, and there is a sharp decline in the breakdown strength as the object approaches the ground plane.

From this preliminary investigation, two main observations have been made. Firstly, the effect of polarity in a gap with a floating conductor is hugely significant, with an opposite effect on the breakdown strength being observed. Secondly, the consequence of the severe decline in breakdown strength of a negative DC gap as a FC approaches the ground plane is that the low field area close to the tower or earth of a negative DC line is very likely an area of concern for live-line maintenance on DC lines.

Although this work only considered relatively small air gaps when compared to the physical size of air gaps between HVDC transmission line components, it was proposed that the polarity dependant results from the presented work can be applied to larger air gaps due to the fact that streamer formation forms the early part of the leader mechanism which dominates breakdown of larger gaps.

REFERENCES

[1] E. F. Raynham, *Apollo - Cahora Bassa: Enigma and Diversions*. EE Publishers, 2004.

[2] Enhanced access to electricity for Southern Africa - the Caprivi Interconnector. European Commision. Last accesed: 3 May 2012. [Online]. Available: http://ec.europa.eu/europeaid/what/energy/sustainable/cs_caprivi_en.htm

[3] Eskom, "Transmission ten year development plan: 2012 - 2021," 2011.

[4] A. Britten, L. Pillay, P. Naidoo, F. Bologna, D. Muftic, and N. Ijumba, "Eskom's proposed strategic research into HVDC transmission," Energize, July 2005.

[5] "IEEE guide for maintenance methods on energized power lines," *IEEE Std 516-2009*, pp. 1 – 143, 24 2009.

[6] E. Kuffel, W. Zaengl, and J. Kuffel, *High Voltage Engineering: Fundamentals*, 2nd ed. Newnes, 2000.

[7] F. Rizk, "Effect of floating conducting objects on critical switching impulse breakdown of air insulation," in *IEEE Transactions on Power Delivery*, vol. 10, no. 3, July 1995, pp. 1360–1370.

[8] B. Hutzler, "Switching impulse strength of air gaps containing a metallic body at floating potential," in *Fifth International Symposium on High Voltage Engineering*, 1987.

[9] G. Baldo and G. Pesavento, "Floating potential bodies and discharge characteristics," in *Seventh International Symposium on High Voltage Engineering*, 1991.

[10] Task Force 07.02 of CIGRE Study Committee 33: Britten, Fonseca, Garbagnati, Hutzler, Zheng-Jianchao, "Strength of external insulation during live line maintenance and repair work with special reference to transient overvoltages," *Electra*, vol. 129, pp. 108–131, March 1990.

[11] "High voltage test techniques - Part 1: General definitions and test requirements," *IEC 60060-1*, 2010.

[12] C. Hart, K. Nixon, and I. Jandrell, "Initial research into quantifying the effect of a sustained dc field on breakdown phenomena using high-speed photography," in *Proceedings for the 17th International Symposium on High Voltage Engineering*, 2011.

[13] L. Niemeyer, L. Ullrich, and N. Wiegart, "The mechanism of leader breakdown in electronegative gases," *IEEE Transactions on Electrical Insulation Vol. 24 No. 2, April 1989*, vol. 24, no. 2, pp. 309 – 324, April 1989.

Appendix E

Conference submission to GD 2012

A paper by the author that is based on the presented work is included. This paper was presented at Gas Discharges (GD) 2012.

THE EFFECT OF A FLOATING CONDUCTOR ON THE NEGATIVE DC BREAKDOWN STRENGTH OF A NON-UNIFORM GAP

C L HART[1], K J NIXON[1] AND I R JANDRELL[1],

[1]School of Electrical and Information Engineering, University of the Witwatersrand, South Africa.
craig.hart@students.wits.ac.za

ABSTRACT

This paper presents a preliminary investigation into the effect of a floating conductor on the breakdown strength of a negative DC rod-plane gap, in order to model the case of live-line maintenance on a negative HVDC line. The experimental work determines the U_{50} breakdown voltage of a rod-plane gap as the floating conductor is moved within the gap. With the study performed in Johannesburg at an altitude of 1732 m, the experimental work looks specifically at the effect of a floating conductor in the case of reduced air density. A comparison of the change in the breakdown strength of the gap is made against the base case of a rod-plane gap with no object and a gap size which is equal to the total gap size minus the floating conductor. The U_{50} breakdown voltage is then presented as a function of the primary gap (energised rod to floating conductor) length. From the results of two different gap sizes, the presence of a floating conductor immediately lowers the breakdown strength of the gap, and there is a sharp decline in the breakdown strength as the object approaches the ground plane. At two positions in the experiments with the larger gap size, two distinct levels of a U_{50} breakdown voltage were found. The occurrence of the two different levels was linked to a difference in the observed corona preceding breakdown.

1. INTRODUCTION

There is currently a growing interest and large development in High Voltage Direct Current (HVDC) power transmission in Africa. The number of proposed HVDC projects worldwide, as well as in Africa, is due to the favourability of HVDC technology in transmitting over long distances when compared to High Voltage Alternating Current (HVAC) [1]. Renewable energy projects, such as hydroelectric plants and wind farms are proposed and constructed in specific locations due to prevailing conditions, which results in vast distances between the generation and load. As an example, the distance to import power to South Africa from the Inga hydroelectric project would in the Democratic Republic of the Congo (DRC) in Central Africa require close to 4000 km of transmission line, which is only realistically feasible if it is HVDC [1].

The unique and challenging aspect of HVDC power transmission is the fact that the electric field around the line's conductor is very different, and much less understood, than that of High Voltage Alternating Current (HVAC) transmission lines. This is due to the constant electric field resulting from a DC voltage in comparison to the alternating field resulting from an AC voltage. While the field conditions surrounding HVAC lines have been extensively researched, this is not the case for HVDC lines. With HVDC lines, there are three types of configurations, namely monopolar, bipolar and homopolar. With these three types of configurations, the conductors can be at either positive or negative polarity, or a conductor at each polarity as in the case of bipolar lines [2]. This then leads to HVDC lines with a constant negative field as well as lines with a constant positive electric field, resulting in a sustained field at both polarities. The polarity of the DC voltage also has an effect on the field distortion due to the behaviour of the space charge in a reversed field [3], leading to an increased number of factors which must be investigated in order to better understand HVDC transmission.

This paper presents a preliminary investigation into the scenario of live-line maintenance on negative HVDC lines by looking at the effect of a floating conductor on the negative DC breakdown strength of a non-uniform gap.

Furthermore, the experimental work presented was performed in Johannesburg at an altitude of 1732 m, meaning that the research specifically models the scenario of this live-line maintenance in conditions of reduced air density.

2. BACKGROUND

Worldwide, many power utilities perform live-line maintenance on their power transmission and distribution networks in order to minimise line downtime and maximise power throughput on the network. As it stands, the IEEE standard for live-line maintenance does not differentiate between the requirements for live-line maintenance on AC or DC lines [4]. This aspect of power transmission, because of the aforementioned different field conditions around DC lines, would have to be adapted for it to be safely performed on HVDC lines. This would mean investigating the effect of a live-line worker entering a non-uniform electric field created by the HVDC line, such as between an energised DC line and a tower.

Previous research on live-line maintenance has focussed on the investigation of switching impulse conditions. Rizk [5], Hutzler [6], and Baldo and Pesavento [7] all modelled the scenario of live-line maintenance using a Floating Conductor (FC) in a non-uniform gap. This successfully models several cases of live-line maintenance, most importantly a worker on metal platform, a worker in a conductive suit or an approaching helicopter. In all these cases, a conductor at floating potential is introduced into an air gap between the line and tower geometry.

3. EXPERIMENTAL PROCEDURE

3.1. Experimental set-up

In order to model the scenario of live-line maintenance, a FC is inserted into a non-uniform field. For all the tests performed in this study, a 150 mm diameter copper sphere with a 100 mm protrusion was employed. The geometrical specifications of the sphere are based on past research on floating body potentials and their effect on the breakdown strength of a non-uniform gap [6]. From the conclusions of this work, a sphere with an anodic protrusion is chosen as the FC that would represent the most onerous case of a floating object in an electric field.

The protrusion used in combination with the sphere is a 5 mm diameter square-cut rod. The FC is orientated such that it has an anodic protrusion because if this is not the case, the protrusion does not have any additional effect towards the FC's decay of the breakdown strength of the gap [6]. This conclusion is from work that did not consider negative polarity however it is assumed that the conclusion is consistent for both polarities. The test set-up is shown in Fig. 1, where d_1 and d_2 represent the primary and secondary gaps respectively. The combination of the two gaps is referred to as the split gap.

The experimental set-up consists of a rod-plane gap with the FC suspended within this gap. The gap is energised using a 320 kV limited DC generator with a rated maximum current of 15 mA. All experimental work was done in the High Voltage Laboratory at the University of the Witwatersrand in Johannesburg in reduced air density conditions at an altitude of 1732 m.

3.2. Experimental procedure

The experimental procedure is based on the determination of the U_{50} breakdown voltage of a rod-plane gap with a FC for different positions of the FC within the gap, using the IEC standard for HVDC testing [8]. The U_{50} breakdown voltage is determined by linearly increasing a DC voltage until breakdown occurs and the breakdown voltage being noted. This is repeated a minimum of five times for each specific set-up, with the average value giving the U_{50} breakdown voltage. The presence of the FC within the test object means that the FC must be earthed after every application of a shot in order to discharge any floating charge on the object.

The position of the object is identified by either the size of the primary gap (d_1) or the percentage ratio of the primary gap to the split gap ($d_1 + d_2$). For consistency, the position of the FC will be referred to by the latter. The variation of the position of the FC in the test gap is shown in Fig. 2, where the position of the conductor is moved in increments of 12.5%. A base case for comparison of the results is a rod-plane gap with no object and a gap size equal to the split gap size. This is based on the fact that the presence of

a FC effectively short circuits the gap over its length in the rod-plane gap.

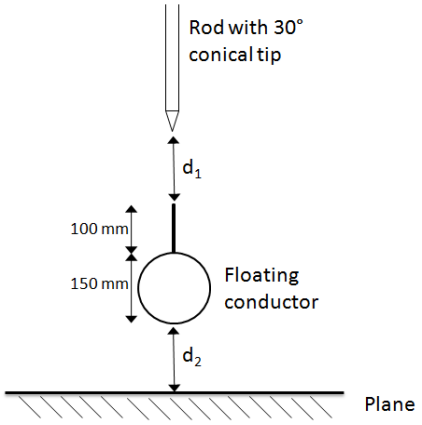


Fig. 1: Diagram of the test object used for the experimental work with a negative DC voltage

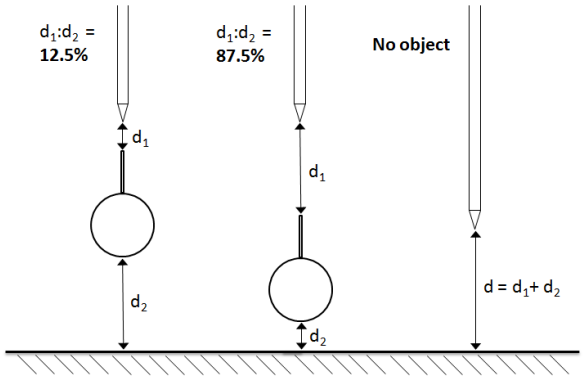


Fig.2: *Test procedure for determination of the breakdown strength of a gap with a floating conductor*

4. RESULTS AND ANALYSIS

4.1. Overview of results

This experimental work consists of two different gap sizes in order to obtain a more general view of the effect of the FC on the breakdown strength of the test gap, with split gap sizes of 17.5 cm and 25 cm respectively. These gap sizes are used as they correspond to breakdown voltages at the limit of the generator's capability. Initial work was done with a 17.5 cm split gap with only three positions of the FC at 25%, 50% and 75%. In experimental work with the 25 cm split gap, the position of the FC was varied from 12.5% to 82.5% in 12.5% increments. The U_{50} breakdown voltage as a function of the primary gap length for both the 17.5 cm and 25 cm split gap sizes is presented in Figs. 3 and 4 respectively. Note that the data point when the primary gap is zero represents the no object case.

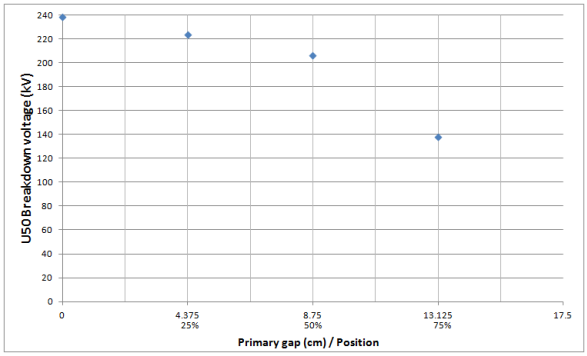


Fig. 3: *U_{50} breakdown voltage of a negative DC rod-plane gap with a floating conductor and a split gap size of 17.5 cm*

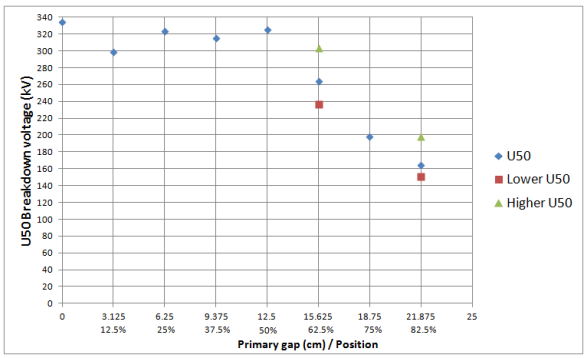


Fig. 4: *U_{50} breakdown voltage of a negative DC rod-plane gap with a floating conductor and a split gap size of 25 cm*

4.2. Discussion of results

Figs. 3 and 4 show the effect of the position of the FC along the central axis on the breakdown strength of a rod-plane gap energised by a negative direct voltage for a 17.5 cm and 25 cm split gap respectively. From both Figs. 3 and 4, there is an evident decline in the breakdown strength of both test gaps as the FC approaches the ground plane. It is also evident that the breakdown strength of the negative DC gap is immediately lowered by the presence of the FC within the gap regardless of its position.

In Fig. 4, the breakdown strength trend of the gap slightly zig-zags prior to a severe decline after the 50% position of the FC. The reason for this is not clear, however it should be noted that during the negative DC tests, there was a high degree of movement of both the rod and the charged FC within the sustained electric field, most likely due to their interaction with the field.. These small degrees of movements will have an effect on the presumably sensitive primary gap made up of a rod-protrusion gap.

Another observation from the experiments is that two positions in the 25 cm tests (62.5% and 82.5%) had results which showed two distinct levels in the U_{50} test, from an increased total of ten shots, as is shown in Fig. 4. A clear observation made at these two positions was that the level (upper or lower) at which breakdown occurred was highly dependent on the observed corona. Prior to breakdown at the higher level, intermediate audible and visual corona would subside before a second, more intense amount of audible and visible corona would occur, directly preceding breakdown of the gap. Breakdown at the lower levels in these positions did not have this second, more intense occurrence of corona, and shortly after the voltage at which corona subsided, breakdown would occur. Interpretation of this phenomenon is ongoing and will be reported in due course.

A similar observation was made by Baldo and Pesavento [7], where they observed two distributions of values for breakdown probability. The range between the two levels was dependant on the length and capacitance of the secondary gap, with an increase in range as the secondary gap was increased. This work, however, was for switching impulses and so the effect of corona could not be observed as the voltage was not being raised like it was in the presented work.

5. CONCLUSION

Experimental work was conducted to investigate the effect of a FC on the breakdown strength of a negative DC gap. A FC comprising of a sphere and anodic protrusion was chosen based on previous research on floating bodies. From the results, it was evident that the presence of a FC immediately lowers the breakdown strength of the gap, compared to the equivalent no-object case. It was also observed that for both split gap sizes, the breakdown strength of the gap decreases as the object approaches the ground plane, with a severe decline after the 50% position.

Additionally, at two positions of the floating object in the experimental work with the split gap size of 25 cm, two distinct levels of the U_{50} breakdown voltage were observed. The behaviour of the corona just prior to the breakdown at both levels was noticeably different and therefore a link between these two observations is possible.

REFERENCES

[1] A. Britten, L. Pillay, P. Naidoo, F. Bologna, D. Muftic, and N. Ijumba, “Eskom’s proposed strategic research into HVDC transmission,” Energize, July 2005.

[2] N. Ijumba and G. Sibilant, The planning, design and construction of overhead powerlines. Crown Publications cc, February 2005, ch. 4, pp. 68–92.

[3] E. Kuffel, W. Zaengl, and J. Kuffel, High Voltage Engineering: Fundamentals, 2nd ed. Newnes, 2000.

[4] “IEEE guide for maintenance methods on energized power lines,” IEEE Std 516-2009, pp. 1 – 143, 24 2009.

[5] F. Rizk, “Effect of floating conducting objects on critical switching impulse breakdown of air insulation,” in IEEE Transactions on Power Delivery, vol. 10, no. 3, July 1995, pp. 1360–1370.

[6] B. Hutzler, “Switching impulse strength of air gaps containinga metallic body at floating potential,” in Fifth International Symposium on High Voltage Engineering, 1987.

[7] G. Baldo and G. Pesavento, “Floating potential bodies and discharge characteristics,” in Seventh International Symposium on High Voltage Engineering, 1991.

[8] “High voltage test techniques - Part 1: General definitions and test requirements,” IEC 60060-1, 2010.